

**İSTANBUL TECHNICAL UNIVERSITY ★ INSTITUTE OF SCIENCE AND TECHNOLOGY**

**EFFECT OF TIME INTEGRATION SCHEMES ON THE LINEAR  
TRANSIENT ANALYSIS OF COMPOSITE PLATES**

**M.Sc.Thesis by  
Kıvanç ŞENGÖZ, B.Sc.**

**Department: Mechanical Engineering  
Programme: Solid Mechanics**

**JUNE 2006**

**EFFECT OF TIME INTEGRATION SCHEMES ON THE LINEAR  
TRANSIENT ANALYSIS OF COMPOSITE PLATES**

**M.Sc.Thesis by  
Kıvanç ŞENGÖZ, B.Sc.  
(503021520)**

**Date of submission : 08 May 2006  
Date of defence examination: 16 June 2006**

**Supervisor (Chairman): Assoc. Prof. Dr. Erol ŞENOCAK**

**Members of the Examining Committee: Prof. Dr. Mehmet DEMİRKOL**

**Prof. Dr. Zahit MECİTOĞLU**

## **ACKNOWLEDGMENTS**

I would like to thank my supervisor Assoc.Prof.Dr. Erol Şenocak for his help and patience throughout thesis.

I would also like to thank all others who contributed to this thesis. In particular, I wish to thank Cem Celal Tulum, Hakan Tanrıöver, Gökmen Aksoy, Kadir Elitok for providing useful comments and help.

Sincere thanks go to my mother and brother for their never ended supports.

To the memory of my father,

May 2006

Kıvanç ŞENGÖZ

## **TABLE OF CONTENTS**

<b>ABBREVIATIONS</b>	<b>IV</b>
<b>LIST OF TABLES</b>	<b>V</b>
<b>LIST OF FIGURES</b>	<b>VI</b>
<b>LIST OF SYMBOL</b>	<b>VIII</b>
<b>ÖZET</b>	<b>IX</b>
<b>SUMMARY</b>	<b>X</b>
<b>1. INTRODUCTION</b>	<b>1</b>
1.1 Scope of Work	2
<b>2. MECHANICS OF LAMINATED COMPOSITE PLATES</b>	<b>3</b>
2.1 Engineering Constants of Orthotropic Materials	4
2.2 Constitutive Relations for Plane Stress	5
2.3 Coordinate Transformation For Laminates	6
2.4 Classical and First Order Theories of Laminated Composite Plates	7
2.5 Displacement , Strain and Constitutive Equations For The Laminated Composite Plates	9
<b>3. NAVIER SOLUTIONS FOR CROSS PLY LAMINATED COMPOSITE PLATES</b>	<b>13</b>
3.1 General Remarks About The Navier Solution	13
3.2 Spatial Variation of The Solution For Classical and Shear Deformable Plates	15
<b>4. BASICS OF THE TRANSIENT DYNAMIC ANALYSIS</b>	<b>19</b>
4.1 General Remarks About Transient Dynamic Problems	19
4.2 Governing Equations For Structural Dynamics	20
4.3 Direct Time Integration methods	21
4.3.1 Central Difference Scheme	24
4.3.2 Houbolt Scheme	26
4.3.3 Newmark Scheme	27
<b>5. LINEAR TRANSIENT DYNAMIC APPLICATION ON CROSS PLY COMPOSITE PLATE</b>	<b>30</b>
5.1 Effect of Time Integration Schemes On Cross Ply Composite Plate	33
5.2 Effect of Plate Theories On The Transient Response	38
5.3 Verification of Transient Code with Sample Literature Problems and geometric nonlinearity effect in plates.	48
<b>6. CONCLUSIONS AND RECOMMENDATIONS</b>	<b>49</b>
<b>REFERENCES</b>	<b>51</b>
<b>BIBLIOGRAPHY</b>	<b>53</b>

## **ABBREVIATIONS**

<b>CSPT</b>	: Classical Plate Theory
<b>SHDT</b>	: Shear Deformation Theory
<b>FEM</b>	: Finite Element Method
<b>FEA</b>	: Finite Element Analysis
<b>FSP</b>	: Finite Strip Method

## LIST OF TABLES

<b>Table 5.1</b>	Comparison of Matlab navier solution and Abaqus fem solution	33
<b>Table 5.2</b>	Effect of Implicit constant average acceleration scheme on the transient response of cross ply plate.....	36
<b>Table 5.3</b>	Effect of time integration with Explicit central difference.....	38
<b>Table 5.4</b>	Effect of time integration with Houbolt implicit scheme.....	38
<b>Table 5.5</b>	Effect of classical plate theory on the response of two layer cross ply plate.....	41
<b>Table 5.6</b>	Effect of shear deformation theory on the response of two layer cross ply plate.....	42
<b>Table 5.7</b>	Effect of layers and shear deformation on the center transverse deflection.....	42

## LIST OF FIGURES

<b>Figure 2.1</b>	: Schematic of laminas and laminate in composite plate.....	3
<b>Figure 2.2</b>	: Kinematics of plate theories.....	8
<b>Figure 2.3</b>	: Force , Moment Resultants & Laminate Coordinate system .....	11
<b>Figure 4.1</b>	: Errors due to direct numerical integration.....	25
<b>Figure 4.2</b>	: Effect of time integration schemes on the period elongation.....	29
<b>Figure 4.3</b>	: Numerical Damping Ratios For Different Schemes.....	29
<b>Figure 4.4</b>	: Effect of different Newmark $\beta$ parameters on period elongation..	30
<b>Figure 5.1</b>	: Unit step loading.....	32
<b>Figure 5.2</b>	: Code accuracy referenced to Reddy's solution.....	33
<b>Figure 5.3</b>	: Central Transverse displacement comparison of implicit and explicit schemes with time step 1 microsecond.....	34
<b>Figure 5.4</b>	: Central Transverse acceleration comparison of implicit and explicit schemes with time step 1 microsecond.....	34
<b>Figure 5.5</b>	: Transverse displacement comparison of implicit and explicit schemes with time step 5 microsecond.....	35
<b>Figure 5.6</b>	: Central transverse acceleration comparison of implicit and explicit schemes with time step 5 microsecond.....	35
<b>Figure 5.7</b>	: Effect of time steps of implicit trapezoidal method on transverse displacement.....	36
<b>Figure 5.8</b>	: Effect of time steps of implicit trapezoidal method on transverse displacement.....	37
<b>Figure 5.9</b>	: Unstability behaviour of central difference method with time step 6 microseconds.....	37
<b>Figure 5.10</b>	: Effect of Houbolt time integration on transient response.....	39
<b>Figure 5.11</b>	: Effect of numerical damping of Houbolt time integration scheme	39
<b>Figure 5.12</b>	: Effect of numerical damping of Houbolt time integration scheme at time step 10 microseconds.....	40
<b>Figure 5.13</b>	: Center normal stress for classical and shear deformation theory	40
<b>Figure 5.14</b>	: Center transverse displacement for classical and shear deformation theory.....	41
<b>Figure 5.15</b>	: Uniformly distributed blast pressure - time history for isotropic plate.....	43
<b>Figure 5.16</b>	: Blast Pressure versus time for sample problem of Chen .....	44
<b>Figure 5.17</b>	: Response of isotropic plate to blast pressure central deflection...	45
<b>Figure 5.18</b>	: Chen's [20] linear and nonlinear displacmenet results with finite element and finite strip method .....	45
<b>Figure 5.19</b>	: Response of isotropic plate to blast pressure central in plane stress.....	45
<b>Figure 5.20</b>	: Chen's [20] linear and nonlinear stress results with finite element and finite strip method.....	46
<b>Figure 5.21</b>	: Central transverse displacement response of one layer orthotropic plate subject to uniform step loading.....	47

<b>Figure 5.22</b>	: Chen's linear and nonlinear displacement results with finite element and finite strip method for the response of one layer orthotropic plate .....	48
<b>Figure 5.23</b>	: Central in plane stress of one layer orthotropic plate subject to uniform step loading.....	48
<b>Figure 5.24</b>	: Chen's [20] linear and nonlinear results with finite element and finite strip method for the response of one layer orthotropic plate to uniform step loading.....	49



## LIST OF SYMBOLS

$a, b$	: side lengths of the plate
$A$	: Extensional stiffness
$B$	: Bending-Extensional coupling stiffness
$C$	: Damping coefficient
$D$	: Bending stiffness
$E$	: Young's modulus
$F$	: Force
$h$	: plate thickness
$I$	: Inertia
$G$	: Shear modulus
$k$	: Shear coefficient
$K$	: Bending curvature
$M_{ij}$	: Elements of Mass matrix
$M_i$	: Moment resultants
$N$	: Force resultants
$P$	: Load
$Q$	: Stiffness coefficients
$t$	: time
$u$	: displacement in the x direction
$v$	: displacement in the y direction
$V, \Delta$	: general displacements
$\nu_{ij}$	: poisson ratio for the ij direction
$\rho$	: density
$\varepsilon$	: Strain
$\sigma$	: Stress
$\theta$	: Ply angle
$\beta, \gamma$	: Newmark Integration Parameters
$\psi$	: Rotation
$\omega$	: natural frequency
$w$	: displacement in the z direction
$z$	: distance from the midplane

## **ZAMAN İNTEGRASYON YÖNTEMLERİNİN KOMPOZİT PLAKALARIN DOĞRUSAL ZAMANA BAĞLI ANALİZLERİ ÜZERİNDEKİ ETKİLERİ**

### **ÖZET**

Bu çalışmada sırasıyla 0 ve 90 derecelik fiber yönlendirmesine sahip iki tabakalı elastik kompozit bir plakanın basit mesnetli sınır koşulları altında, zamana bağlı ve sinuzoidal dağılımlı yükleme altında, yer değiştirme uzayında analitik çözümü belirlenmiş ve zaman bağlı analiz için gerekli adi diferansiyel denklem takımı elde edilmiştir. Çözüm için diferansiyel denklem takımı numerik olarak zaman boyutunda direk integrasyon teknikleri kullanarak integre edilmiş ve üç farklı integrasyon metodunun zamana bağlı davranış üzerindeki etkileri belirlenmiştir. Gerekli seri çözümü ve adi diferansiyel denklemin zaman boyunca integre edilmesi işlemleri Matlab yazılımı kullanarak programlanmış ve plaka merkezi üzerindeki düşey deplasman ve düzlem içi gerilmeler sunulmuştur. Ayrıca klasik ve birinci dereceden plaka teorileri de programlanarak sonuç üzerindeki etkileri incelenmiştir. Elde edilen sonuçlarda Newmark kapalı zaman integrasyon metodu olan trapez metod, zaman uzayındaki cevabın belirlenmesinde numerik stabilite ve hassasiyet açısından diğer metodlara göre daha iyi yaklaşımlar yapmıştır. Houbolt metodu ve merkezi farklar yöntemi daha büyük zaman adımlarında istenilen çözüm hassasiyetinden sapmalar göstermiştir. Houbolt metodu kısa süreli ani dinamik yükleme içeren problemlerde iyi sonuçlar üretemeyen bir kapalı zaman integrasyonu olarak gözlemlenmiştir. Açık direk integrasyon tekniği olan merkezi farklar yöntemi koşullu numerik stabilite nedeniyle belirli bir zaman adımı büyüklüğünü geçtikten sonra ( 5 mikrosaniye üzerinde ) sonsuza giden sonuçlar vermiş ve bu yönden problemli bir integrasyon tekniği olarak değerlendirilmiştir. Plaka kenar uzunluğu kalınlık oranının 5 olduğu bir durum için kayma etkisini gözönünde bulunduran plaka teorisi ile elde edilen deplasman sonuçları klasik teori ile bulunan sonuçlardan yüzde otuz farklı elde edilmiştir. Klasik teori kayma etkilerini gözönünde bulundurmadiğı için deplasman ve gerilme cevabını gerçek değerinin altında hesaplayabilmiş, plaka frekansını ise olması gereken cevabın üstünde hesaplamıştır.

## **EFFECT OF TIME INTEGRATION SCHEMES ON THE LINEAR TRANSIENT ANALYSIS OF COMPOSITE PLATE**

### **SUMMARY**

For cross ply composite plate with two layers, under appropriate boundary conditions and sinusoidal distribution of the transverse load with step loading, the exact form of the spatial variation of the solution is obtained and the problem is reduced to the solution of a system of ordinary equations in time, which are integrated numerically using direct integration methods. Effect of time integration schemes on linear elastic dynamic response of the composite plate is investigated considering implicit dynamic schemes average acceleration, Houbolt and explicit scheme central difference. Necessary code for the solution of linear transient analysis of composite plates was programmed in Matlab considering the procedure outlined above. Furthermore influence of classical and first order theories are addressed for transient dynamic response and included as different matlab codes. Numerical results for the central deflection and center in plane stress are presented for comparison with the aim of the code. The results clearly show that trapezoidal implicit method ( Newmark method with  $\gamma=0.5$  and  $\beta=0.25$  ) has better approximation in time space in terms of accuracy and stability. In Houbolt scheme and explicit central difference scheme deviation from the accuracy of the solutions were observed at larger time steps compared with trapezoidal method. Houbolt is inappropriate time integration technique for short duration dynamic problems. Although explicit scheme has good correlation at smaller time steps, it suffers instability with time steps larger than 5 microseconds. So conditional stability of this method is important problem at these time steps. In the considered length to thickness (  $a/h=5$  ) ratio, thirty percentage of difference was observed in displacement response when shear deformation theory is used in plate behaviour. Although this ratio is so severe classical plate theory under predict the displacement and stress response while over predict the frequency of the response.

## 1. INTRODUCTION

With the increased application of composites in high performance aircraft, studies involving the assessment of the transient response of the laminated composite plate are receiving attention. Composite plates are susceptible to low velocity (150 ft/sn) impact as transient loads such as dropped tools, runway stones and tire blow out debris. Relatively thick layered composite plates also have significant armor applications and are exposed to explosive and nuclear blast transient loading with high load intensity in short durations. Also the need for more profound understanding of the response of laminated composites arises from potential use of such materials in jet engine fan and compressor blades which are vulnerable to impact of foreign objects. The linear elastic transient response of isotropic plates has been investigated by several researchers. Reissman and his colleagues [3] analysed a simply supported rectangular isotropic plate subject to a suddenly applied load, uniformly distributed load over a rectangular area. Exact solution was obtained using classical three dimensional elasticity theory and classical and improved theories. Hinton and his associates [4] presented transient finite element analysis of thick and thin isotropic plates.

Layered composite plates exhibit general coupling between the inplane displacements and the transverse displacements and shear rotations. Consequently, the response of composite plates is sensitive to the lamination scheme. Also due to low transverse shear deformation effects are more pronounced in composites than in isotropic plates. Moon [13] has investigated the response of infinite laminated plates subjected to the transverse impact load at the center of the plate. Chow [17] has employed the Laplace transform technique to investigate the dynamic response of the orthotropic laminated plates. Sun and his colleagues [10] have employed the classical method of separation of variables with the Mindlin - Goodman procedure for treating time dependent boundary conditions and dynamic loadings. Anderson and Madenci [7] presented analytical solution of finite geometry composite plates under transient surface loading including material damping.

## 1.1 Scope of Work

It is clear that transient simulation of composite plates with the explicit finite element codes has provided useful information to the researchers as a new trend. Ease of implementation of the complex contact algorithms, nonlinear material properties and damage models in explicit codes has accelerated their usage in last years. On the other hand drawback of this time integration method is the stability problem due to nature of the finite difference time integration scheme and sensitivity degree of response to chosen time step more than implicit methods have. Therefore in this work nature of the time integration schemes trapezoidal method of Newmark - Beta, Houbult and central difference on the transient response of composite plates is investigated. Also stability, time step sensitivity, amplitude decay and period elongation issues are addressed. This will enable researchers to decide on certain attributes of time integration choice for transient response of composite plates. During that response importance of plate theory used in the formulation for the kinematics of the plate is another scope especially in the transverse deformation of plates. At this point impact of classical and first order shear deformation theories on transverse deflection and inplane stress is investigated to shed light on the importance of theories for the kinematics of plate deformation.

## 2.MECHANICS OF THE LAMINATED COMPOSITE PLATES

Basic block of the laminated composites is a lamina or ply. It is the typical sheet of composite material. Fibre- reinforced lamina consist of many fibers embedded in a matrix material. Unidirectional fiber –reinforced lamina exhibit the highest strength and modulus in the direction of the fibers but they have very low strength and modulus in the direction transverse to fibers.

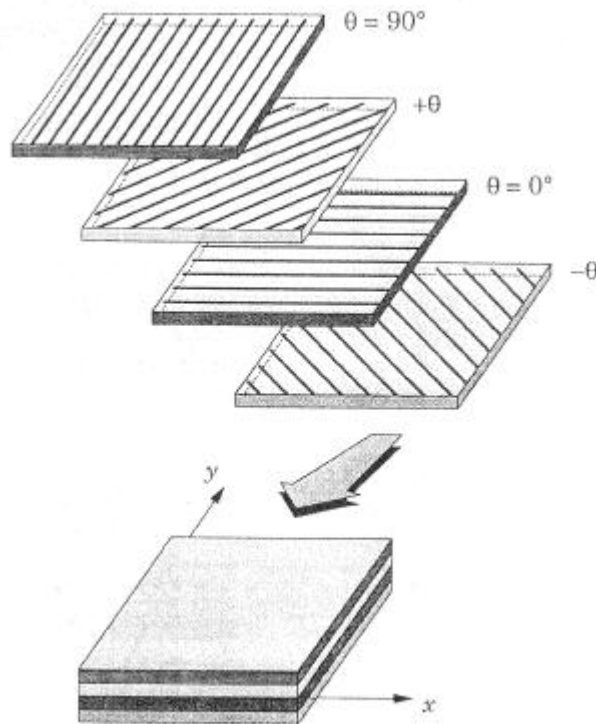


**Figure 2.1** Laminas and laminate for composite plate [2]

A laminate is a collection of laminate stacked to achieve the desired stiffness and thickness. The sequence of various orientations of a fiber reinforced composite layer in a laminate is termed lamination scheme or stacking sequence. Unidirectional fiber – reinforced laminate (all lamina have the same fiber orientation) will be very strong along the direction of the fibers but weak in transverse direction. The laminate will be weak in shear also. If laminate has layers with fibers oriented at

30 or 45 degrees, it can take shear loads. Laminated composite structures also have disadvantages. Because of the material properties between layers, the shear stresses produced between layers, especially at the edges of a laminate, may cause delamination [2].

## 2.1 Engineering Constants of Orthotropic Materials

The constitutive equations for a material which has three orthogonal planes of material property symmetry characterized by nine independent material properties. Fourth order tensor with fully anisotropic tensor has 81 constants.

$$\sigma_{ij} = E_{ijkl} \varepsilon_{ij} \quad (2.1)$$

with strain symmetry arguments reduced 36 constants and including thermodynamic considerations set up 21 constants and orthotropic symmetry argument result in 9 constants.

$$\begin{Bmatrix} \sigma_{11} \\ \sigma_{22} \\ \sigma_{33} \\ \sigma_{12} \\ \sigma_{13} \\ \sigma_{23} \end{Bmatrix} = \begin{bmatrix} Q_{11} & Q_{12} & Q_{13} & & & \\ & Q_{12} & Q_{22} & Q_{23} & & \\ & Q_{13} & Q_{23} & Q_{33} & & \\ & & & & Q_{44} & \\ & & & & & Q_{55} \\ & & & & & & Q_{66} \end{bmatrix} \begin{Bmatrix} \varepsilon_{11} \\ \varepsilon_{22} \\ \varepsilon_{33} \\ \varepsilon_{12} \\ \varepsilon_{13} \\ \varepsilon_{23} \end{Bmatrix} \quad (2.2)$$

In this case the material stiffness coefficients  $Q_{ij}$  can be expressed in terms of engineering constants  $E_1, E_2, E_3, G_{12}, G_{23}, G_{13}, \nu_{12}, \nu_{23}, \nu_{13}$ . These constants are measured using simple tests like uniaxial tension or pure shear [2].

## 2.2 Constitutive Relations for Plane Stress

A plane stress state is defined to be one in which all transverse stresses are negligible. Most laminates are typically thin and experience a plane state of stress. For lamina in the  $x_1, x_2$  plane, the transverse stress components are  $\sigma_{33}, \sigma_{13}, \sigma_{23}$ . Although these stress components are in small comparison to  $\sigma_{11}, \sigma_{12}, \sigma_{22}$  they can induce failures because fiber reinforced composite laminates are weak in the transverse direction (because the strength providing fibers are in the transverse  $x_1, x_2$  plane). Thus the transverse stress components are not always neglected in the

laminate analyses. However whenever they are neglected in a laminate theory, the constitutive equations must be modified to account for the fact that

$$\sigma_{33}=0, \sigma_{44}=0, \sigma_{55}=0, \text{ and } \sigma_{13}=0, \sigma_{23}=0, \sigma_{43}=0, \sigma_{53}=0, \quad (2.3)$$

So stress-strain relations take the form

$$\begin{Bmatrix} \sigma_1 \\ \sigma_2 \\ \sigma_3 \end{Bmatrix} = \begin{bmatrix} Q_{11} & Q_{12} & 0 \\ Q_{12} & Q_{22} & 0 \\ 0 & 0 & Q_{66} \end{bmatrix} \begin{Bmatrix} \varepsilon_1 \\ \varepsilon_2 \\ \varepsilon_3 \end{Bmatrix} \quad (2.4)$$

$Q_{ij}$  called the plane stress-reduced stiffnesses are given by

$$\begin{aligned} Q_{11} &= \frac{E_1}{1 - \nu_{12}\nu_{21}} \\ Q_{12} &= \frac{E_2\nu_{12}}{1 - \nu_{12}\nu_{21}} \\ Q_{22} &= \frac{E_2}{1 - \nu_{12}\nu_{21}} \\ Q_{66} &= G_{12} \end{aligned} \quad (2.5)$$

Note that reduced stiffness involve four independent material constants  $E_1, E_2, \nu_{12}, G_{12}$ . When the normal stress is neglected but the transverse shear stresses are included equation 2.3 should be appended with the constitutive relations.

$$\begin{Bmatrix} \sigma_4 \\ \sigma_5 \end{Bmatrix} = \begin{bmatrix} Q_{44} & 0 \\ 0 & Q_{55} \end{bmatrix} \begin{Bmatrix} \varepsilon_4 \\ \varepsilon_5 \end{Bmatrix}, \quad Q_{44} = G_{23} \quad Q_{55} = G_{13} \quad (2.6)$$

### 2.3 Coordinate Transformations For Laminate

Since the laminate is made up of several orthotropic layers (laminas), with their material axes oriented arbitrarily with respect to the laminate coordinates, the constitutive equations of each layer must be transformed from lamina coordinates  $x_1, x_2, x_3$  to the laminate coordinates  $x, y, z$ .

$$\begin{Bmatrix} \sigma_{xx} \\ \sigma_{yy} \\ \sigma_{xy} \end{Bmatrix}^k = \begin{bmatrix} \bar{Q}_{11} & \bar{Q}_{12} & \bar{Q}_{16} \\ \bar{Q}_{12} & \bar{Q}_{22} & \bar{Q}_{26} \\ \bar{Q}_{16} & \bar{Q}_{26} & \bar{Q}_{66} \end{bmatrix}^k \begin{Bmatrix} \varepsilon_{xx} \\ \varepsilon_{yy} \\ \gamma_{xy} \end{Bmatrix}^k \quad (2.7)$$



$$\begin{Bmatrix} \sigma_{xz} \\ \sigma_{yz} \end{Bmatrix}^k = \begin{bmatrix} \bar{Q}_{44} & \bar{Q}_{45} \\ \bar{Q}_{45} & \bar{Q}_{55} \end{bmatrix}^k \begin{Bmatrix} \gamma_{yz} \\ \gamma_{xz} \end{Bmatrix}^k \quad (2.7)$$

Where  $k$  specifies the layer and  $Q_{ij}$ 's are elements of the transformation matrix depend on ply angle of  $k^{\text{th}}$  layer ( fiber orientation) .

$$\begin{aligned} \bar{Q}_{11} &= Q_{11} \cos^4\theta + 2 (Q_{12} + 2 Q_{66}) \sin^2\theta \cos^2\theta + Q_{22} \sin^4\theta \\ \bar{Q}_{12} &= (Q_{11} + Q_{22} - 4Q_{66}) \sin^2\theta \cos^2\theta + 2 (Q_{12} \sin^4\theta \cos^4\theta) \\ \bar{Q}_{22} &= Q_{11} \sin^4\theta + 2 (Q_{12} + 2 Q_{66}) \sin^2\theta \cos^2\theta + Q_{22} \cos^4\theta \\ \bar{Q}_{16} &= (Q_{11} - Q_{12} - 2Q_{66}) \sin^2\theta \cos^3\theta + 2 (Q_{12} \sin^4\theta \cos^4\theta) \\ \bar{Q}_{26} &= (Q_{11} - Q_{12} - 2Q_{66}) \sin^3\theta \cos\theta + 2 (Q_{12} - Q_{22} + 2Q_{66}) \\ \bar{Q}_{66} &= (Q_{11} + Q_{22} - 2Q_{12} - 2Q_{66}) \sin^2\theta \cos^2\theta + Q_{66} (\sin^4\theta + \cos^4\theta) \\ \bar{Q}_{44} &= (Q_{44} \cos^2\theta + Q_{55} \sin^2\theta), \bar{Q}_{45} = (Q_{55} - Q_{44}) \cos\theta \sin\theta \\ \bar{Q}_{55} &= (Q_{55} \cos^2\theta + Q_{44} \sin^2\theta) \\ \bar{Q}_{45} &= (Q_{55} - Q_{44}) \cos\theta \sin\theta \\ \bar{Q}_{55} &= (Q_{55} \cos^2\theta + Q_{44} \sin^2\theta) \end{aligned} \quad (2.8)$$

## 2.4 Classical and First Order Theories of Laminated Composite Plates

Classification of Structural Laminate Plate theories

(1) Equivalent single –layer theory ( ESL) ( 2-D)

a ) Classical laminate theory

b ) Shear deformation and higher order laminated theories. For example Reddy's third order theory [2].

(2) Three dimensional elasticity theory (3-D)

a ) Traditional 3-D elasticity formulations

b ) Layerwise theories

(3) Multiple model methods (2-D and 3-D)

The equivalent single layer (ESL) theories are derived from the 3-D elasticity theory by making suitable assumptions concerning the kinematics of deformation or the stress state through the thickness of the laminate. These assumptions allow the

reduction of the problem to 2-D problem. In the three dimensional elasticity theory or in a layerwise theory, each layer is modelled as 3-D solid.

Composite laminates are formed by stacking layers of different composite materials and fiber orientation. By construction, composite laminates have their planar dimensions one or two orders of magnitude larger than their thickness. Often laminates are used in applications that require axial and bending strengths. Therefore composite laminates are treated as plate elements.

The simplest plate theory is the classical laminate plate theory (CLPT) which is an extension of the Kirchhoff (classical) plate theory to the laminated composite plates. It is based on the displacement field [2].

$$\begin{aligned} u_1(x; y; z; t) &= u(x; y; t) - z^* \partial w / \partial x \\ u_2(x; y; z; t) &= v(x; y; t) - z^* \partial w / \partial y \\ u_3(x; y; z; t) &= w(x; y; t) \end{aligned} \quad (2.9)$$

(u,v,w) are the displacements components along the (x,y,z) coordinate directions. The displacement field implies that straight lines normal to the xy plane before deformation remain straight and normal to the midsurface after deformation. The Kirchhoff assumption amounts to neglecting both transverse shear and transverse normal effects, deformation is entirely due to bending and in plane stretching.

The next theory is the first order shear deformation theory (FSDT) which is based on the displacement field [2].

$$\begin{aligned} u_1(x; y; z; t) &= u(x; y; t) + z^* \psi_x(x; y; t) \\ u_2(x; y; z; t) &= v(x; y; t) + z^* \psi_y(x; y; t) \\ u_3(x; y; z; t) &= w(x; y; t) \end{aligned} \quad (2.10)$$

here t is the time  $u_1, u_2, u_3$  are the displacements in x, y, z directions respectively  $u, v, w$  are the associated midplane displacements and  $\psi_x$  and  $\psi_y$  are the slopes in xz and yz planes due to bending only. The FSDT extends the kinematics of the CLPT by including a gross transverse shear deformation in its kinematics assumptions, the transverse shear strain is assumed to be constant with respect to the

thickness coordinate. Inclusion of this form shear deformation allows the normality restriction of the classical laminate theory to be relaxed. The first order shear deformation theory requires shear correction factors which are difficult to determine for arbitrary laminated composite plate. The shear factor depends not only on the lamination and geometric parameters, but also loading and boundary conditions.

In both CLPT and FSDT, the plane stress state assumption is used and plane-stress reduced form of the constitutive is used. In both theories the inextensibility and straightness of transverse normals can be removed. Such extensions lead to second and higher order theories [2].

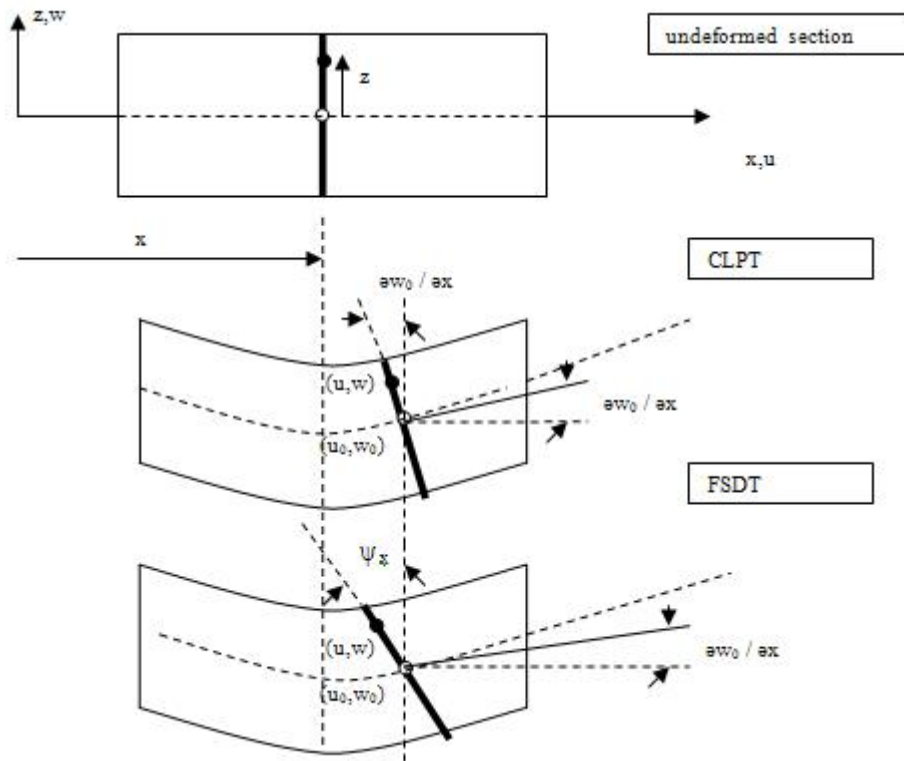


**Figure 2.2** Kinematics of plate theories [2].

In addition to their inherent simplicity and low computational cost, the ESL models often provide sufficiently accurate description of global response for thin to moderately thick laminates such as gross deflections, critical buckling loads and fundamental vibration frequencies and associated mode shapes. Of the ESL theories, the FSDT with transverse extensibility appears to provide the best compromise of solution accuracy, economy, and simplicity. However The ESL models have limitations that prevent them from being used to solve the whole spectrum of composite laminate problems. First accuracy of the global response predicted by

the ESL models deteriorates as the laminate becomes thicker. Second the ESL models are often in capable of accurately describing the state of stress and strain at the ply level near geometric and material discontinuities or near regions of intense loading – the areas where accurate stresses are needed most.

## 2.5 DISPLACEMENT, STRAIN AND CONSTITUTIVE EQUATIONS FOR THE LAMINATED COMPOSITE PLATES

For CLPT following Kirchhoff hypothesis holds. Straights lines perpendicular to the midsurface (transverse normals) before deformation remain straight after deformation. The transverse normals do not experience elongation (they are inextensible). The transverse normals rotate such that they remain perpendicular to the midsurface after deformation. The first two assumptions imply that the transverse displacement is independent of the transverse coordinate and the transverse normal strain  $\varepsilon_{zz}$  is zero. The third assumption results in zero transverse shear strains. In the formulations layers are perfectly bonded together and each layer is of uniform thickness. The strains associated with the displacement field can be computed using either nonlinear- strain displacement relations or the linear strain displacement relations. General form of nonlinear strains [2]

$$\begin{aligned}
 E_{xx} &= \left( \frac{\partial u}{\partial x} \right) + 0.5 * \left[ \left( \frac{\partial u}{\partial x} \right)^2 + \left( \frac{\partial v}{\partial x} \right)^2 + \left( \frac{\partial w}{\partial x} \right)^2 \right] \\
 E_{yy} &= \left( \frac{\partial v}{\partial y} \right) + 0.5 * \left[ \left( \frac{\partial u}{\partial y} \right)^2 + \left( \frac{\partial v}{\partial y} \right)^2 + \left( \frac{\partial w}{\partial y} \right)^2 \right] \\
 E_{zz} &= \left( \frac{\partial w}{\partial z} \right) + 0.5 * \left[ \left( \frac{\partial u}{\partial z} \right)^2 + \left( \frac{\partial v}{\partial z} \right)^2 + \left( \frac{\partial w}{\partial z} \right)^2 \right] \\
 E_{xy} &= 0.5 * \left[ \left( \frac{\partial u}{\partial y} \right) + \left( \frac{\partial v}{\partial x} \right) \right] + 0.5 * \left[ \left( \frac{\partial u}{\partial x} \right) \left( \frac{\partial u}{\partial y} \right) + \left( \frac{\partial v}{\partial x} \right) \left( \frac{\partial v}{\partial y} \right) + \left( \frac{\partial w}{\partial x} \right) \left( \frac{\partial w}{\partial y} \right) \right] \\
 E_{xz} &= 0.5 * \left[ \left( \frac{\partial u}{\partial z} \right) + \left( \frac{\partial w}{\partial x} \right) \right] + 0.5 * \left[ \left( \frac{\partial u}{\partial x} \right) \left( \frac{\partial u}{\partial z} \right) + \left( \frac{\partial v}{\partial x} \right) \left( \frac{\partial v}{\partial z} \right) + \left( \frac{\partial w}{\partial x} \right) \left( \frac{\partial w}{\partial z} \right) \right] \\
 E_{yz} &= 0.5 * \left[ \left( \frac{\partial v}{\partial z} \right) + \left( \frac{\partial w}{\partial y} \right) \right] + 0.5 * \left[ \left( \frac{\partial u}{\partial y} \right) \left( \frac{\partial u}{\partial z} \right) + \left( \frac{\partial v}{\partial y} \right) \left( \frac{\partial v}{\partial z} \right) + \left( \frac{\partial w}{\partial y} \right) \left( \frac{\partial w}{\partial z} \right) \right]
 \end{aligned} \tag{2.11}$$

If the components of the displacements gradients are of the order of  $\mathcal{E}$  then the small strain assumptions implies that the terms of the order  $\mathcal{E}^2$  are negligible in the strains. If the rotations  $\partial w / \partial x$  and  $\partial w / \partial y$  of transverse normals are moderate ( say  $10^\circ$  or  $15^\circ$  ) then  $\mathcal{E}^2$  terms of these terms are small but not negligible compared to  $\mathcal{E}$  so they should be included in strain displacement equation. In this case small strain with moderate rotations is special from of the geometric nonlinearity and this form of strains named Von Karman strains and theory is the Von Karman plate theory. In most simple form with linear strain and displacement assumption and If we assume that total strain is made up of in plane stretching  $\varepsilon_i^0$  and bending  $K_i$  strains also known as curvatures

$$\begin{Bmatrix} \varepsilon_{11} \\ \varepsilon_{22} \\ \varepsilon_{12} \end{Bmatrix} = \begin{Bmatrix} \varepsilon^0_1 \\ \varepsilon^0_2 \\ \varepsilon^0_6 \end{Bmatrix} + z \begin{Bmatrix} K_1 \\ K_2 \\ K_6 \end{Bmatrix} \quad (2.12)$$

Where

$$\begin{aligned} \varepsilon^0_1 &= \left( \frac{\partial u}{\partial x} \right) , \quad \varepsilon^0_2 = \left( \frac{\partial v}{\partial y} \right) , \quad \varepsilon^0_6 = \left( \frac{\partial v}{\partial y} \right) + \left( \frac{\partial u}{\partial x} \right) \\ K_1 &= \left( -\frac{\partial^2 w}{\partial x^2} \right) , \quad K_2 = \left( -\frac{\partial^2 w}{\partial y^2} \right) , \quad K_6 = \left( -2 \frac{\partial^2 w}{\partial y \partial x} \right) \end{aligned} \quad (2.13)$$

Stress strain relationship [2]

$$\begin{Bmatrix} \sigma_{11} \\ \sigma_{22} \\ \sigma_{12} \end{Bmatrix}^k = \begin{bmatrix} \bar{Q}_{11} & \bar{Q}_{12} & \bar{Q}_{16} \\ \bar{Q}_{12} & \bar{Q}_{22} & \bar{Q}_{26} \\ \bar{Q}_{16} & \bar{Q}_{26} & \bar{Q}_{66} \end{bmatrix}^k \begin{Bmatrix} \varepsilon_{11} \\ \varepsilon_{22} \\ \varepsilon_{12} \end{Bmatrix}^k \quad (2.14)$$

Force and moment resultants [2]

$$\begin{Bmatrix} N_{11} \\ N_{22} \\ N_{12} \end{Bmatrix} = \sum_{k=1}^m \int_{z_k}^{z_{k+1}} \begin{Bmatrix} \sigma_{11} \\ \sigma_{22} \\ \sigma_{12} \end{Bmatrix} dz = \sum_{k=1}^m \int_{z_k}^{z_{k+1}} \begin{bmatrix} \bar{Q}_{11} & \bar{Q}_{12} & \bar{Q}_{16} \\ \bar{Q}_{12} & \bar{Q}_{22} & \bar{Q}_{26} \\ \bar{Q}_{16} & \bar{Q}_{26} & \bar{Q}_{66} \end{bmatrix}^k \left[ \begin{Bmatrix} \varepsilon^0_1 \\ \varepsilon^0_2 \\ \varepsilon^0_6 \end{Bmatrix} + z \begin{Bmatrix} K_1 \\ K_2 \\ K_6 \end{Bmatrix} \right] dz \quad (2.15)$$

$$\begin{Bmatrix} N_{11} \\ N_{22} \\ N_{12} \end{Bmatrix} = \begin{bmatrix} A_{11} & A_{12} & A_{16} \\ A_{12} & A_{22} & A_{26} \\ A_{16} & A_{26} & A_{66} \end{bmatrix} \begin{Bmatrix} \varepsilon^0_1 \\ \varepsilon^0_2 \\ \varepsilon^0_6 \end{Bmatrix} + \begin{bmatrix} B_{11} & B_{12} & B_{16} \\ B_{12} & B_{22} & B_{26} \\ B_{16} & B_{26} & B_{66} \end{bmatrix} \begin{Bmatrix} K_1 \\ K_2 \\ K_6 \end{Bmatrix} \quad (2.16)$$

m is the number of layer of the plate for the equation 2.15 and 2.16.

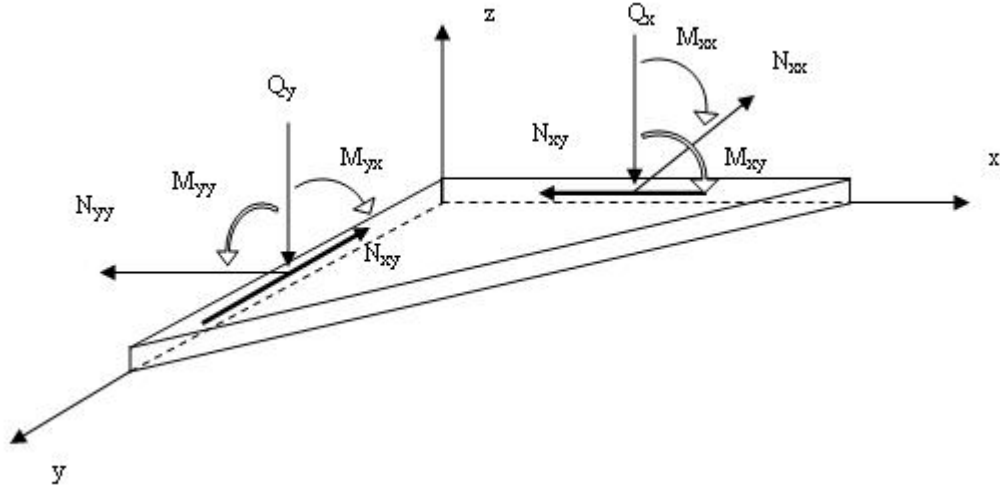


**Figure 2.3** Force, Moment Resultants.

$$\begin{pmatrix} M_{11} \\ M_{22} \\ M_{12} \end{pmatrix} = \sum_1^m \int_{z_k}^{z_{k+1}} \begin{Bmatrix} \sigma_{11} \\ \sigma_{22} \\ \sigma_{12} \end{Bmatrix} z dz = \sum_1^m \int_{z_k}^{z_{k+1}} \begin{bmatrix} \bar{Q}_{11} & \bar{Q}_{12} & \bar{Q}_{16} \\ \bar{Q}_{12} & \bar{Q}_{22} & \bar{Q}_{26} \\ \bar{Q}_{16} & \bar{Q}_{26} & \bar{Q}_{66} \end{bmatrix}^k \begin{Bmatrix} \varepsilon^0_1 \\ \varepsilon^0_2 \\ \varepsilon^0_6 \end{Bmatrix} + z \begin{Bmatrix} K_1 \\ K_2 \\ K_6 \end{Bmatrix} z dz \quad (2.17)$$

$$\begin{pmatrix} M_{11} \\ M_{22} \\ M_{12} \end{pmatrix} = \begin{bmatrix} B_{11} & B_{12} & B_{16} \\ B_{12} & B_{22} & B_{26} \\ B_{16} & B_{26} & B_{66} \end{bmatrix} \begin{Bmatrix} \varepsilon^0_1 \\ \varepsilon^0_2 \\ \varepsilon^0_6 \end{Bmatrix} + \begin{bmatrix} D_{11} & D_{12} & D_{16} \\ D_{12} & D_{22} & D_{26} \\ D_{16} & D_{26} & D_{66} \end{bmatrix} \begin{Bmatrix} K_1 \\ K_2 \\ K_6 \end{Bmatrix} \quad (2.18)$$

$A_{ij}$  is called extensional stiffnesses,  $D_{ij}$  the bending stiffnesses and  $B_{ij}$  the bending extensional coupling stiffnesses.

$$(A_{ij}, B_{ij}, D_{ij}) = \sum_1^m \int_{z_m}^{z_{m+1}} (1, z, z^2) * Q_{ij}^{(m)} dz \quad (2.19)$$

In the case of FSDT, the kirchoff hypothesis is relaxed by removing the third part, transverse normals do not remain perpendicular to the midsurface after deformation. This amounts including transverse shear strains in the theory. The inextensibility of

transverse normals requires that  $w$  not be a function of the thickness coordinate.

Assuming displacement field [2]

$$\begin{aligned} u_1(x; y; z; t) &= u(x; y; t) + z^* \psi_x(x; y; t) \quad , \quad \frac{\partial u}{\partial z} = \psi_x \\ u_2(x; y; z; t) &= v(x; y; t) + z^* \psi_y(x; y; t) \quad , \quad \frac{\partial v}{\partial z} = \psi_y \\ u_3(x; y; z; t) &= w(x; y; t) \end{aligned} \quad (2.20)$$

Also note that  $\varepsilon_{33}$  is zero is due to inextensibility of transverse normal.

$$\begin{Bmatrix} \varepsilon_{11} \\ \varepsilon_{22} \\ \varepsilon_{23} \\ \varepsilon_{13} \\ \varepsilon_{12} \end{Bmatrix} = \begin{Bmatrix} \varepsilon^0_1 \\ \varepsilon^0_2 \\ \varepsilon^0_4 \\ \varepsilon^0_5 \\ \varepsilon^0_6 \end{Bmatrix} + z \begin{Bmatrix} K_1 \\ K_2 \\ K_4 \\ K_5 \\ K_6 \end{Bmatrix} \quad (2.21)$$

$$\varepsilon^0_5 = \left( \frac{\partial w}{\partial x} \right) + \psi_x \quad , \quad \varepsilon^0_4 = \left( \frac{\partial w}{\partial y} \right) + \psi_y \quad (2.22)$$

Also  $\varepsilon^0_1, \varepsilon^0_2, \varepsilon^0_3$  have the the same description with CLPT

$$\begin{aligned} K_1 &= \left( \frac{\partial \psi_x}{\partial x} \right) \quad , \quad K_2 = \left( \frac{\partial \psi_y}{\partial y} \right) \quad , \quad K_6 = \left( \frac{\partial \psi_x}{\partial y} \right) + \left( \frac{\partial \psi_y}{\partial x} \right) \\ K_4 &= 0 \quad , \quad K_5 = 0 \end{aligned} \quad (2.23)$$

And same form of Inplane force resultants and moment resultants are holds for FSDT.

For  $i, j=1,2,6$  Moment and Force resultants takes general form as shown below.

$$\begin{Bmatrix} N_i \\ M_i \end{Bmatrix} = \begin{bmatrix} A_{ij} & B_{ij} \\ B_{ij} & D_{ij} \end{bmatrix} \begin{Bmatrix} \varepsilon_j \\ K_j \end{Bmatrix} \quad (2.24)$$

$$(A_{ij}, B_{ij}, D_{ij}) = \sum_1^m \int_{z_m}^{z_{m+1}} (1, z, z^2)^* Q_{ij}^{(m)} dz \quad (2.25)$$

In addition to this, transverse force resultants  $Q_i$  for  $i = 4,5$

$$\begin{Bmatrix} Q_4 \\ Q_5 \end{Bmatrix} = \begin{bmatrix} \bar{A}_{44} & \bar{A}_{45} \\ \bar{A}_{45} & \bar{A}_{55} \end{bmatrix} \begin{Bmatrix} \varepsilon_4 \\ \varepsilon_5 \end{Bmatrix} \quad (2.26)$$

$$\bar{A}_{ij} = \sum_m \int_{z_m}^{z_{m+1}} (k_i * k_j) * Q_{ij}^{(m)} dz \quad (2.27)$$

and  $k$  is the shear coefficient.



### 3. NAVIER SOLUTIONS FOR CROSS PLY LAMINATED COMPOSITE PLATES

In this thesis, the navier solution method is used to determine the spatial variation of the transient solution .Thus typical dependent variable is expanded as

$$a(x,y,t) = \sum_{m,n} H_{m,n}(t) \phi(x,y) \quad (3.1)$$

where  $H_{mn}$  are suitable functions of  $t$  that satisfy the boundary conditions and  $H_{mn}$  are coefficients to be determined such that  $a(x,y,t)$  satisfies its governing equation. The choice of a separable solution form as above implies that the general spatial variation is independent of time and its amplitude varies with time.

#### 3.1 General Remarks For The Navier Solution

In the Navier method the generalized displacements are expanded in double trigonometric series in terms of the unknown parameters. The choice of functions in the series is restricted to those which satisfy the boundary conditions of the problem. Substitution of the displacements expansions into the governing equations should result in a unique set of algebraic equations among the parameters of the expansion. The Navier solutions can be developed for rectangular laminates with two sets of boundary conditions. Even for these boundary conditions, not all laminates permit the solution

Equation of motion for SHDT in the presence of applied transverse forces,  $q$  as

$$\begin{aligned}
N_{1,x} + N_{6,y} &= I_0 * u_{,tt} + I_1 * \psi_{x,tt} \\
N_{6,x} + N_{2,y} &= I_0 * v_{,tt} + I_2 * \psi_{y,tt} \\
Q_{4,x} + Q_{5,y} &= I_0 * w_{,tt} + q(x,y,t) \\
M_{1,x} + M_{6,y} - Q_4 &= I_2 * \psi_{x,tt} + I_1 * u_{,tt} \\
M_{6,x} + M_{2,y} - Q_5 &= I_2 * \psi_{y,tt} + I_1 * v_{,tt} \\
\partial M_1 / \partial x_i &= M_{1,x} \quad , \quad \partial^2 u / \partial t^2 = u_{,tt}
\end{aligned} \tag{3.2}$$

Where P, R and I are the normal, coupled normal-rotary and rotary inertia coefficients.

$$(P, R, I) = \int_{-h/2}^{h/2} (1, z, z^2) * \rho dz = \sum_m \int_{z_m}^{z_{m+1}} (1, z, z^2) * \rho^{(m)} dz \tag{3.3}$$

Using the Constitutive equations 2.20, equations of the motions 3.2 could be expressed in terms of the displacements as follows [1].

$$[L]\{\lambda\} = \{f\} + [M]\{\ddot{\lambda}\} \quad , \quad \{\lambda\} = [u, v, w, \psi_x, \psi_y]^T \tag{3.4}$$

$$\begin{aligned}
L_{11} &= A_{11} d_{11} + 2 A_{16} d_{12} + A_{66} d_{22} + P d_{tt} \\
L_{12} &= (A_{11} + A_{66}) d_{12} + A_{16} d_{22} + A_{26} d_{22}, \quad L_{13} = 0 \\
L_{14} &= (B_{11} d_{11} + 2 B_{16} d_{12} + B_{66} d_{22} + R d_{tt} \\
L_{15} &= (B_{12} d_{11} + B_{66}) d_{12} + B_{26} d_{22} = L_{24} \\
L_{25} &= 2 B_{26} d_{12} + B_{22} d_{22} + B_{66} d_{11} + R d_{tt} \\
L_{22} &= A_{22} d_{22} + 2 A_{26} d_{12} + A_{66} d_{tt} + P d_{tt} \\
L_{33} &= -A_{44} d_{11} - 2 A_{25} d_{12} - A_{55} d_{22} + P d_{tt} \\
L_{34} &= A_{44} d_1 - A_{55} d_2, \quad L_{35} = -A_{45} d_1 - A_{55} d_2 \\
L_{44} &= D_{11} d_{11} + 2 D_{16} d_{12} + D_{66} d_{22} - A_{44} + I d_{tt} \\
L_{45} &= (D_{12} + D_{16}) d_{12} + D_{16} d_{11} + D_{26} d_{22} - I d_{tt} - A_{45} \\
L_{45} &= 2 D_{16} d_{12} + D_{22} d_{22} + D_{66} d_{tt} + I d_{tt} - A_{55}
\end{aligned} \tag{3.5}$$

Where  $d_i = \partial / \partial x_i$   $d_{ij} = \partial^2 / \partial x_i \partial x_j$  ( $i = j = 1, 2$ ) and  $d_{tt} = \partial^2 / \partial t^2$

$$M_{11} = M_{22} = M_{33} = P, \quad M_{44} = M_{55} = R \quad (3.6)$$

$$M_{ij} = 0 \text{ for } i \neq j \text{ (} i, j = 1, 2, \dots, 5 \text{)}$$

$$F_3 = q \quad \text{and} \quad F_1 = F_2 = F_4 = F_5 = 0$$

### 3.2 Exact Form Of The Spatial Variation of The Solution

The boundary initial- value problem associated with the forced motions of the layered anisotropic composite plate involves solving the equation 3.3 subjected to a given set of boundary and initial conditions. It is not possible to construct exact solutions to equation 3.4 when the plate is of arbitrary geometry, constructed arbitrarily oriented layers and subject to an arbitrary loading and boundary conditions. However an exact form of the spatial variation of the solution to equation 3.4 can be developed for two different lamination schemes and associated boundary conditions, when the plate is of rectangular geometry and subjected to sinusoidally distributed with respect to  $x$ , and  $y$  arbitrary with respect to time transverse loading.

Considering the following simply supported boundary conditions.

$$x = 0, a \quad v = w = \psi_y = 0 \quad ; \quad N_1 = 0 \quad M_1 = 0 ;$$

$$y = 0, b \quad u = w = \psi_x = 0 \quad ; \quad N_6 = 0 \quad M_2 = 0 ;$$

The following form of the solution satisfies the boundary conditions

$$\begin{aligned} u &= \sum_{m,n} U_{m,n}(t) \phi_1(x, y), \quad v = \sum_{m,n} V_{m,n}(t) \phi_2(x, y), \quad w = \sum_{m,n} W_{m,n}(t) \phi_3(x, y), \\ \psi_x &= \sum_{m,n} X_{m,n}(t) \phi_1(x, y), \quad \psi_y = \sum_{m,n} Y_{m,n}(t) \phi_2(x, y), \end{aligned} \quad (3.7)$$

Where

$$\phi_1 = \cos \alpha x \sin \beta y, \quad \phi_2 = \cos \beta x \sin \alpha y, \quad \phi_3 = \cos \beta y \sin \alpha x \quad (3.8)$$

Substituting equation 3.7 into equation 3.4 we find that solution to equation to 3.4 exist when the transverse loading is of the form

$$q(x, y, t) = \sum_{m,n} Q_{m,n}(t) \phi_3(x, y),$$

$$Q_{mn}(t) = \frac{4}{ab} \int_0^a \int_0^b q(x, y, t) \sin(m\pi x/a) \sin(n\pi y/b) \quad (3.9)$$

and the lamination scheme is such that ( which correspond to cross play lamination scheme )

$$A_{16} = A_{26} = A_{45} = B_{16} = B_{26} = D_{16} = D_{26} = 0 \quad (3.10)$$

Under these conditions equation 3.3 becomes

$$[M] \{ \ddot{\Delta} \} + [C] \{ \dot{\Delta} \} = \{ F \} \quad (3.11)$$

Thus for a given  $\alpha = m\pi/a$  ,  $\beta = n\pi/b$  where a and b side lengths of the rectangular plate where

$$\{ \Delta \} = \{ U_{mn}, V_{mn}, W_{mn}, X_{mn}, Y_{mn} \}^T$$

$$\{ F \} = \{ 0, 0, Q_{mn}, 0, 0 \}^T \quad (3.12)$$

The elements of symmetric stiffness coefficient matrix based on the first order plate theory [1].

$$C_{11} = A_{11} \alpha^2 + B_{66} \beta^2, \quad C_{12} = (A_{12} + A_{66}) \alpha \beta$$

$$C_{13} = 0$$

$$C_{14} = B_{11} \alpha^2 + B_{66} \beta^2, \quad C_{15} = (B_{12} + B_{66}) \alpha \beta$$

$$C_{22} = A_{66} \alpha^2 + A_{22} \beta^2$$

$$C_{23} = 0, \quad C_{24} = C_{15}, \quad C_{25} = B_{66} \alpha^2 + B_{22} \beta^2 \quad (3.13)$$

$$C_{33} = A_{44} \alpha^2 + A_{55} \beta^2$$

$$C_{34} = \alpha A_{44}, \quad C_{35} = A_{55} \beta$$

$$C_{44} = D_{11} \alpha^2 + D_{66} \beta^2 + A_{55}$$

$$C_{45} = (D_{12} + D_{66}) \alpha \beta, \quad C_{55} = D_{66} \alpha^2 + D_{11} \beta^2 + A_{55}$$

And the elements of mass matrix

$$M_{11} = M_{22} = M_{33} = P$$

$$M_{44} = M_{55} = R \quad (3.14)$$

$$M_{ij} = 0 \text{ for } i \neq j$$

Elements of the force matrix

$$F_3 = Q_{mn} \quad (3.15)$$

$$F_1 = F_2 = F_4 = F_5 = 0$$

The load coefficients for a sinusoidally distributed transverse load

$$q(x,y,t) = H(t) q_0 \sin(\pi x/a) \sin(\pi y/b) \quad (3.16)$$

It is a one term solution (  $Q_{mn} = q_0 H(t)$  and  $m = n = 1$  ) and therefore it is closed form solution. For other types of loads, the Navier solution is a series solution, which can be evaluated for sufficient number of terms in the series. For uniform load terms in the series

$$Q_{mn} = (16 q_0 H(t) / \pi^2 mn) \text{ for } m, n \text{ odd} \quad (3.17)$$

Thus for a given  $\alpha = m\pi/a$  ,  $\beta = n\pi/b$  where a and b are the side lengths of the rectangular plate. We have system of 5 differential equations to be solved in time.

So we need to integrate 5x5 matrix differential equation in time for the vector  $\{\Delta\}$  of the generalized displacements.

Using the same methodology and considering CLPT equation of motion

$$N_{1,x} + N_{6,y} = I_0 \ddot{u}_{,tt} - I_1 \ddot{w}_{,x,tt}$$

$$N_{6,x} + N_{2,y} = I_0 \ddot{v}_{,tt} + I_1 \ddot{w}_{,x,tt}$$

$$M_{1,xx} + 2M_{6,yx} + M_{2,xx} = q(x,y,t) + I_0 \ddot{w}_{,tt} - I_2 [(\ddot{w}_{,xx,tt}) + (\ddot{w}_{,yy,tt})] +$$

$$I_1 [(\ddot{u}_{,x,tt}) + (\ddot{v}_{,y,tt})] \quad (3.18)$$

The elements of symmetric stiffness coefficient matrix based on classical plate theory,

$$\begin{aligned}
C_{11} &= A_{11} \alpha^2 + A_{66} \beta^2, \quad C_{12} = (A_{12} + A_{66}) \alpha \beta \\
C_{13} &= -B_{11} \alpha^3 - (B_{12} + 2B_{66}) \alpha \beta^2 \\
C_{22} &= A_{66} \alpha^2 + A_{22} \beta^2, \quad C_{23} = -(B_{12} + 2B_{66}) \alpha \beta^2 - B_{22} \beta^3 \\
C_{33} &= D_{11} \alpha^4 + 2(D_{12} + 2D_{66}) \alpha^2 \beta^2 + D_{22} \beta^4
\end{aligned} \tag{3.18}$$

and the elements of mass and force matrix

$$\begin{aligned}
M_{11} &= I_0 \\
M_{22} &= I_0, \quad M_{33} = I_0 + I_2(\alpha^2 + \beta^2) \\
F_3 &= Q_{mn}, \quad F_1 = F_2 = F_4 = F_5 = 0
\end{aligned} \tag{3.19}$$

This case we need to integrate 3x3 matrix of differential equation in time. The set of algebraic differential equation for any fixed  $m, n$  can be solved with state-space or modal analysis method. Both methods are algebraically complicated and require determination of eigenvalues and eigenfunctions. Therefore solution of ordinary differential equation in time will be computed by approximate numerical solution considering the integration schemes for second order differential equations. Basically in this numerical integration method, time derivatives are approximated using difference approximations ( or truncated Taylor series ) and therefore solution is obtained only for discrete times and not as a continuous function of time. There are two major steps in the solution process for transient analysis. First assume spatial variation of the displacements and reduce the governing partial differential equations to set of ordinary differential equations in time and solve the ordinary differential equation exactly if possible or numerically.

#### **4. BASICS OF THE TRANSIENT DYNAMIC ANALYSIS**

In many engineering applications of dynamic situations the inclusion of dynamic terms in the analysis of structures is essential. The term dynamic implies that inertia terms must be included in the equations of equilibrium. In static loading, time required to increase the magnitude of the applied load is longer than the period of the lowest vibration mode. However depend on the loading rate, if the time required to increase the magnitude of the applied load from zero to its maximum value is less than half the natural period of the structure, dynamic excitation occurs so inertia effects become important. Examples where such inertia effects are important include the impact loading of the structures due to collision or crash, blast or explosive conditions in which case the loading is of high intensity and is applied for a short period of time ( about microseconds ) and seismic action where the structural loading takes the form of prescribed acceleration history [15].

##### **4.1 General Remarks about Transient Dynamic Problems**

Generally transient dynamic problems are classified depending on the effect of the spectral characteristic of the excitation on the overall structural response, as wave propagation problems and inertial problems.

Wave propagation problems: The wave propagation problems are those in which the behaviour at the wave front is of engineering importance and in such cases it is the intermediate and high frequency structural modes that dominate the response throughout the time span of interest. Problems of that fall into this category are shock response from conventional weapons such as explosive or blast loading and problems in which waves effect such as focussing reflections and diffractions are important [16].

Inertial problems: All dynamic problems which are not wave propagation type can be considered as inertial and here the response is governed by relatively small number

of low frequency modes. Problems of this type are often also called structural dynamic problems [15].

Frequencies and modes refer to the eigenspectrum of the linearized structural dynamics equation. Because of nonlinearities this spectrum can be expected to vary with the state. The qualifiers low and intermediate and high refer to frequencies whose associated wavelengths are much smaller than the characteristic acoustic wavelengths, respectively.

As a broad guideline wave propagation problems are best solved by explicit integration techniques whereas implicit integration techniques are more effective for inertial problems. However, the relative economy of both approaches is also influenced by the topology of the finite element mesh and by the type of computer.

In the last twenty years, significant advances have been made in the development and application of numerical methods to solution of dynamic transient problems. A primary factor in this progress has been the parallel development of large high speed digital computers providing the faster execution times required to make the solution of large engineering problem a feasible proposition. This has resulted in the development of many commercially available codes such as Ansys, Abaqus, Mark, Adina.

## **4.2 Governing Equations for Structural Dynamics**

To solve transient structural or continuum mechanics problems numerically, the governing hyperbolic partial differential equations are first discretized in space. This procedure is called a semidiscretization. The semidiscretization will reduce the problem to a system of ordinary differential equations in time, which in turn must be integrated to complete the solution process.

In dynamic analysis, the governing semi discrete equations of motion are obtained by considering the static equilibrium at time  $t$  which include effects of acceleration, dependent inertia forces and velocity dependent damping forces in addition to the externally applied time dependent load and internal forces due to initial stresses in the system. In essence direct numerical integration is based on two ideas [23].



Firstly, the dynamic equilibrium equations are satisfied at discrete time intervals  $\Delta t$  apart. This means that basically static equilibrium, which includes the effect of inertia and damping forces are sought at discrete time points within the interval of the solution.

Secondly, variation of displacements, velocities and accelerations within each time interval  $\Delta t$  is assumed. Different forms of these assumed variations give rise to different direct integration schemes, each of them has different accuracy, stability and cost.

The available direct procedures can be further subdivided into explicit and implicit methods each of with distinct advantages and disadvantages. Each approach employs difference equivalents to develop recurrence relations which may be used in a step by step computation of the response. The critical parameter in the use of each of these techniques is generally the largest value of the time step which can be used to provide sufficiently accurate results, as this is directly related to the total cost of satisfactory results.

### **4.3 Direct Time Integration Methods**

In direct integration the governing ordinary second order differential equations in time resulting from semi - discretization of the structural system ( for example by means of finite element method) given by equation 3.5 for linear structural dynamic response are integrated using a numerical step by step procedure. The term direct means that prior to numerical integration process no transformation of the equations into different form is carried out. The critical parameter in the use of each of these technique is generally the largest value of the time step which can be used to provide sufficiently accurate results and this is directly related to the total cost of satisfactory analysis.

Explicit methods: This technique employs finite difference methods and is particularly well suited for short duration dynamical problems or wave propagation problems such as structures subject to blast or high velocity impact . In the explicit method the solution at time  $t + \Delta t$  is obtained by considering the equilibrium conditions at time  $t$  and such integration schemes do not require factorization of the

effective stiffness matrix in the step by step solution. Hence the method requires no storage of matrices if diagonal mass matrix is used. Computational cost per time step is generally much less for explicit methods and less storage is required than implicit methods. Operations for the explicit method are relatively few in number and are independent of the finite element mesh band or front width. However, explicit time integration schemes are only conditionally stable and generally require small time steps to be employed to insure numerical instability. Here, the step size restriction is often more severe than accuracy considerations require. This restriction limits the effectiveness of the approach when used to study of dynamic problems of moderate duration, e.g. earthquake response problems. The conditionally stable algorithms require the time step size employed to be inversely proportional to the highest frequency of the discrete system. The explicit methods allow the displacements at the current time step  $t + \Delta t$ , to be found in terms of the known displacements, velocities, and accelerations, at previous time step  $t$ . This enables one to evaluate the material physics which can be used to generate new internal stresses for use in the solution at the next step. Also very complex material models can easily incorporated using this approach.

Implicit methods: This approach has its strength in the capability of treating inertial problems such as low speed impact and seismic problems and modelling of complex structural geometries. In the implicit method the equations for the displacements at the current time step involve the velocities and accelerations at the current step itself,  $t + \Delta t$ . Hence the determination of displacements at  $t + \Delta t$  involves the solution of structural stiffness matrix at every time step. Many implicit methods are unconditionally stable for linear analysis and maximum time step length that can be employed is governed by the accuracy of solution and not by the stability of the integration process. Although the implicit methods usually require considerably more computational effort per time step than explicit methods, the time step may be much larger since it is restricted in size only by accuracy requirements. The time step in most explicit methods on the other hand, is restricted only by numerical stability requirements which may result in a time step much smaller than needed for the requisite accuracy, thus increasing the cost of the accuracy.

Stability aspects: The most significant drawback of the central difference method is its conditional stability. If too large time step is used, exceeding stability limit of the system  $\Delta t > \Delta t_{cr}$  the solution quickly blows up and may reach the overflow limits on the computer so the computation becomes numerically unstable. Time step is limited for stability by

$$\Delta t < \Delta t_{cr} \quad \Delta t_{cr} = 2/\omega_{max} \quad (4.1)$$

for undamped system where  $\omega_{max}$  is the maximum natural frequency of the modelled structure considering

$$[K] - \omega^2 [M] = 0 \quad (4.2)$$

Because of round of errors the practical limit on  $\Delta t$  is roughly 25 % less than  $\Delta t_{cr}$ . In finite element,  $\Delta t_{cr}$  is the time required for an acoustic wave to traverse the element with the least traversal time. For homogenous strain elements, this condition can be rewritten in terms of the acoustic wave speed  $c$  and the element length  $l$  in the form as  $\Delta t_{cr} < l/c$ . This equation corresponds to Courant- Freidrick -Lewy condition that courant number  $r = c \Delta t/l$  be less than unity.

The direct integration begin with some known initial conditions displacements  $V_0$  velocity  $\dot{V}_0$ , or acceleration  $\ddot{V}_0$  at time  $t = 0$ . The integration scheme establishes an approximate solution  $V_1, \dot{V}_1, \ddot{V}_1$  at time  $t = \Delta t$  and so on for  $t = 2\Delta t, 3\Delta t, \dots$  etc.

Each method employs a different assumed variation of displacement velocity and acceleration with in the time interval. The errors involved in the direct integration method may result from truncation, from the use of lower order difference approximations to the derivatives of continuous variables, from numerical instability, from amplification of errors in previous time steps into later time steps and from computational round off.

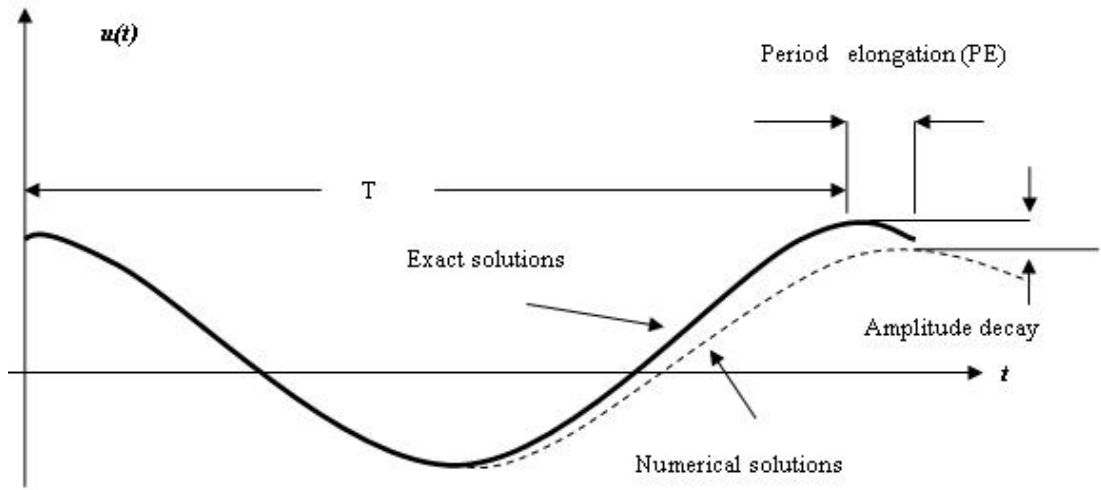


**Figure 4.1** Errors due to direct numerical integration [23]

These errors may introduce a shift in the period and amplitude of the responses which are called period elongation and amplitude decay respectively. The numerical stability of the direct integration method depends on the modal characteristics of the system.

#### 4.3.1 Central Difference Method

In principle, finite difference expression that approximates the acceleration and velocity in terms of the displacements can be used to solve the equation of motion.

$$M\ddot{V} + C\dot{V} + KV = P(t) \quad (4.3)$$

In which the velocity and accelerations are expressed as [6].

$$\dot{V}_n = \frac{1}{2\Delta t} [V_{n+1} - V_{n-1}] , \quad (4.4)$$

$$\ddot{V}_n = \frac{1}{\Delta t^2} [V_{n+1} - 2V_n + V_{n-1}] \quad (4.5)$$

Where subscripts n-1, n, n+1 represent the time at  $(n-1)\Delta t$ ,  $n\Delta t$ , and  $(n+1)\Delta t$  respectively with  $n = 0, 1, 2, \dots$

The displacement at time  $(n+1)\Delta t$  is obtained by considering equation motion at time  $n\Delta t$ ,

$$M\ddot{V}_n + C\dot{V}_n + KV_n = P_n(t) \quad (4.6)$$

Substitute the relations for  $\ddot{V}_n$  and  $\dot{V}_n$  of equation 4.4 and 4.5 into equation 4.5 gives

$$\overline{K} V_{n+1} = P_{n+1} \quad (4.7)$$

Where

$$\begin{aligned} \overline{K} &= \frac{M}{\Delta t^2} + \frac{C}{2\Delta t} \\ P_{n+1} &= P_n - (K - \frac{2M}{\Delta t^2})V_n - (\frac{M}{\Delta t^2} - \frac{C}{2\Delta t})V_{n-1} \end{aligned} \quad (4.8)$$

Note that K is not included in  $\overline{K}$  so there is no need to invert K in central difference method. In these relations the equation for  $V_{n+1}$  involves  $V_n$  and  $V_{n-1}$ . Therefore in order to calculate the solution at the first time step, special starting procedure must be used as shown in equation 4.9

$$V_{-1} = V_0 + \Delta t \dot{V}_0 + 0.5\Delta t^2 \ddot{V}_0 \quad (4.9)$$

Also  $\ddot{V}_0$  can be obtained directly from equation 4.5 using  $V_0$ ,  $\dot{V}_0$  and  $P_0$ .

Considering the single dof system K, C, M and P reduce the k, c, m, p. Rearranging and setting c=0 and p=0,

$$X_{n+1} = [A] X_n \quad (4.10)$$

Where

$$X_{n+1} = \begin{bmatrix} V_{n+1} \\ V_n \end{bmatrix} \quad X_n = \begin{bmatrix} V_n \\ V_{n-1} \end{bmatrix} \quad (4.11)$$

$$A = \begin{bmatrix} 2 - \omega^2 \Delta t^2 & -1 \\ 1 & 0 \end{bmatrix}, \quad \omega^2 = k/m \quad (4.12)$$

Matrix A is called the amplification matrix. Stability and accuracy of an integration algorithm depend on the eigenvalues of this amplification matrix and in order to have a stable solution, the spectral radius, i.e. the maximum eigenvalue of matrix A, has to be smaller than 1. So time step is limited for stability by  $\Delta t < \Delta t_{cr}$  where  $\Delta t_{cr} = 2/\omega_{max}$  for undamped system where  $\omega_{max}$  is the maximum natural frequency

of the modelled structure. In order to have a stable solution using the central difference explicit integration algorithm, time step should be smaller than critical time step. When the frequency gets higher, the allowable time step will decrease. This conditionally stable character is main disadvantage in using explicit central difference method.

#### 4.3.2 Houbolt Method

Houbolt used the following finite difference equations for velocity and accelerations at time  $t = (n+1) \Delta t$

$$\ddot{V}_{n+1} = \frac{1}{\Delta t^2} [2V_{n+1} - 5V_n + 4V_{n-1} - V_{n-2}] \quad (4.13)$$

$$\dot{V}_{n+1} = \frac{1}{6\Delta t} [11V_{n+1} - 18V_n + 9V_{n-1} - 2V_{n-2}] \quad (4.14)$$

These equations were obtained from consideration of a cubic curve that passes through four successive ordinates. In order to obtain solutions at time  $(n+1) \Delta t$  we employ the equations of the motion at time  $(n+1) \Delta t$  and using previous equations for velocity and accelerations we have equation

$$\bar{K} V_{n+1} = \bar{P}_{n+1} \quad (4.15)$$

to solve  $V_{n+1}$  in equation 4.15 we can use equation 4.16 assume that  $(C = 0)$  no physical damping

$$\begin{aligned} \bar{K} &= \frac{M}{dt^2} + K \\ \bar{P}_{n+1} &= P_{n+1} + \left(\frac{5M}{\Delta t^2}\right)V_n - \left(\frac{4M}{\Delta t^2}\right)V_{n-1} + \left(\frac{M}{\Delta t^2}\right)V_{n-2} \end{aligned} \quad (4.16)$$

As with the central difference method, this formulation needs a special starting procedure. Houbolt used the formulas for the derivatives at the third point of the four successive points along the cubic curve. The formulas are given the following values for  $V_{-1}$  and  $V_{-2}$

$$\begin{aligned} V_{-1} &= 2V_0 + \Delta t^2 \ddot{V}_0 - V_1 \\ V_{-2} &= 6\Delta t \dot{V}_0 + 6\Delta t^2 \ddot{V}_0 - 8V_1 + 9V_0 \end{aligned} \quad (4.17)$$

When the same amplification matrix which is 3x3 this case eigenvalues of that matrix always less than 1 so automatically satisfied in every time step chosen. However  $\Delta t$  should be selected in order to achieve proper accuracy. Also note that  $\bar{K}$  include K so inverse of K needed in every time step. This is the characteristic and main disadvantage of implicit methods in terms of solution time and storage requirements.

#### 4.3.3 Newmark Method

In the Newmark method, two parameters  $\lambda$  and  $\beta$  are introduced to indicate how much of the acceleration enters into the relations for velocity and displacement at the end of the time interval. Adopted relations [23]

$$V_{n+1} = \left[ V_n + \Delta t \dot{V}_n + (0.5 - \beta)(\Delta t)^2 \ddot{V}_n + \beta(\Delta t)^2 \ddot{V}_{n+1} \right] \quad (4.18)$$

$$\dot{V}_{n+1} = \left[ \dot{V}_n + (1 - \gamma)\Delta t \ddot{V}_n + \gamma\Delta t \ddot{V}_{n+1} \right]$$

The first equation can be used to express  $\ddot{V}_{n+1}$  in terms of  $\dot{V}_{n+1}$ . Then second substitution of this relationship into second equation gives  $\dot{V}_{n+1}$  in terms of  $V_{n+1}$  then can be obtained by substituting these two relations into the equation of motion at time  $(n+1)\Delta t$ . The result is  $\bar{K} V_{n+1} = \bar{P}_{n+1}$  and assuming  $C=0$

$$\bar{K} = \frac{M}{\beta \Delta t^2} + K \quad (4.19)$$

$$\bar{P}_{n+1} = P_{n+1} + \left(\frac{1}{\beta \Delta t^2}\right)V_n + \left(\frac{1}{\beta \Delta t}\right)\dot{V}_n + \left(\frac{1}{2\beta} - 1\right)\ddot{V}_n$$

Once  $V_{n+1}$  is obtained the corresponding velocity and acceleration vectors can be computed using,

$$\dot{V}_{n+1} = \left[ \dot{V}_n + (1 - \gamma)\Delta t \ddot{V}_n + \frac{\gamma}{\beta} \frac{1}{\Delta t} \left[ V_{n+1} - V_n - (\Delta t)\dot{V}_n - (0.5 - \beta)\Delta t^2 \ddot{V}_n \right] \right] \quad (4.20)$$

$$\ddot{V}_{n+1} = \frac{1}{\beta \Delta t^2} \left[ V_{n+1} - V_n + \Delta t \dot{V}_n + (0.5 - \beta)\Delta t^2 \ddot{V}_n \right]$$

The stability and accuracy of the Newmark method, which is controlled by two parameters  $\beta$  and  $\gamma$ , can be evaluated by examining the eigenvalues associated with the amplification matrix. Method is unconditionally stable for  $\gamma=0.5$  and  $\beta \geq 0.25$ . When  $\gamma=0.5$  and  $\beta = 0.25$  it is known as trapezoidal rule. In trapezoidal rule there is no inherent numerical damping but it has period elongation sensitive the time step chosen on the other hand there is considerable amount of numerical damping for low modes in Houbolt schemes [22].

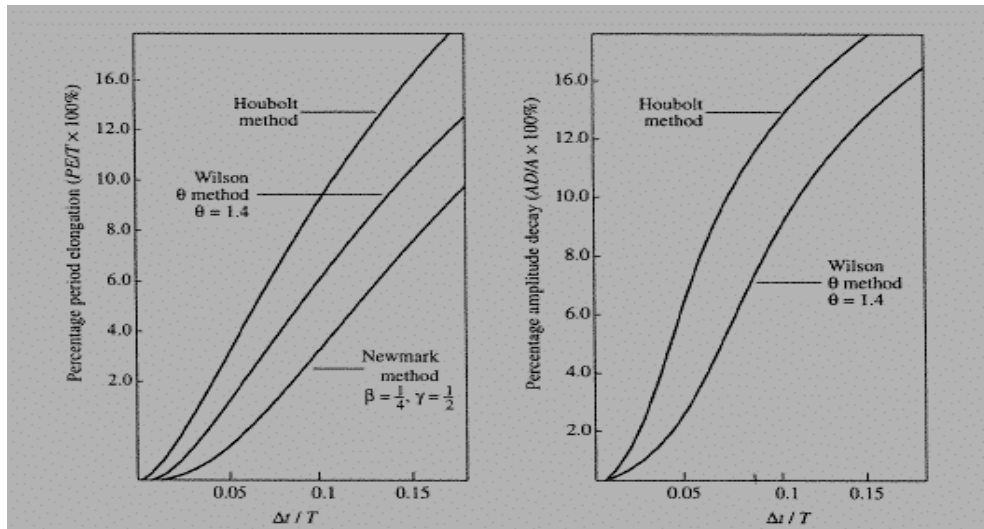


**Figure 4.2** Effect of time integration schemes on the period elongation [21].

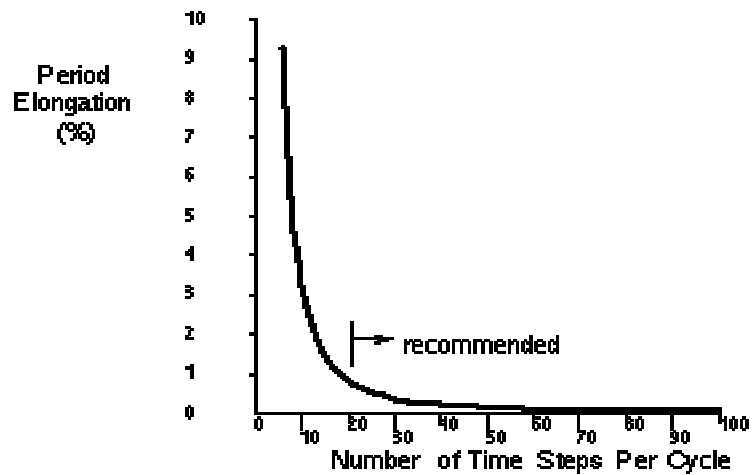


**Figure 4.3** Time step versus period elongation [21].



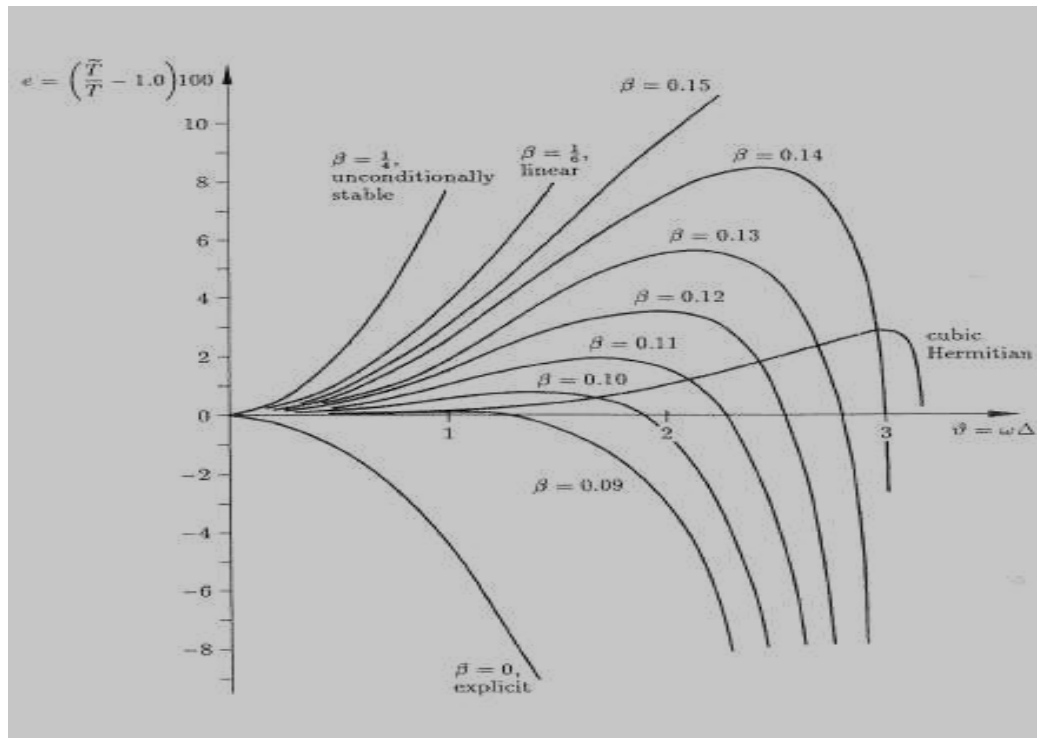


**Figure 4.4** Effect of time integration schemes with different Newmark  $\beta$  parameter on the period elongation versus time step [21].

## 5 . LINEAR TRANSIENT ANALYSIS APPLICATIONS

For the linear transient analysis, Navier solution for the rectangular cross ply composite plate with simply supported boundary conditions was programmed in Matlab. Three different time integration scheme , central difference as explicit scheme, Newmark integration with  $\gamma=0.5$  and  $\beta = 0.25$  which corresponds to average acceleration scheme and Houbolt scheme as implicit schemes were programmed separately to investigate the effect of each scheme on the response. Also classical plate theory and shear deformation theory was programmed separately to observe the effect of shear deformation on the linear transient response. Results of the Matlab code were also verified using the Abaqus commercial finite element code results. Furthermore code was applied to some linear transient problems that were taken from literature and results were compared.

In all numerical examples zero initial conditions for velocity and displacement are assumed. All computations were checked in double precision workstation. The following geometrical and material data for the analysis are used.

$a=b=250 \text{ mm}$   $a/b=1$  : a and b are side lengths of the plate.

$h= 50\text{mm}$  : h is the thickness of the plate.

The material properties for composite plate are as follows.

$E_2 = 2.1 \times 10^6 \text{ N/cm}^2$  : young modulus in the direction transverse to fibers.

$E_1=25 \times E_2$  : young modulus in the fiber direction.

$G_{12}=G_{23}=G_{13}=0.5 \times E_2$  : Shear Modulus

$\nu_{12} = 0.25$  : poison ratio

$\rho = 8 \times 10^{-6} \text{ Nsec}^2/\text{cm}^4$  : density

Loading has sinusoidal distribution in spatial coordinates,

$$q = q_0 \sin(x/a) \sin(y/b) \quad q_0 = 10 \text{ N/cm}^2 \quad (5.1)$$

It is guaranteed that with this load intensity, behaviour of plate response is in linear limits. So there is no considerable deformation compared to thickness of the plate. Thus geometric nonlinearity effect could be excluded with in this load intensity and linearity assumption is reliable. In time, step loading was used for 250 microseconds so general form of the loading is,

$$q(x,y,t) = H(t) q_0 \sin(\pi x/a) \sin(\pi y/b) \quad (5.2)$$

where  $H(t)$  is unit value for 250 microseconds.

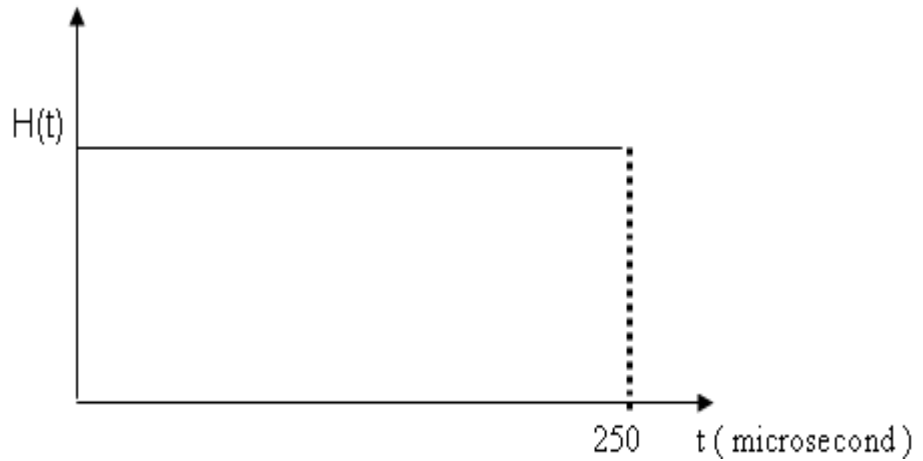


**Figure 5.1** Unit step loading

In table one results with the time step 1 microseconds was presented comparing Abaqus finite element results. In this analysis shear deformation theory was used in two solution. In Abaqus S4R element type was chosen based on SHDT so including shear effects during analysis. Same simple supported boundary conditions and loading type were used in Abaqus and Matlab. Mesh was 20x20 element for rectangular plate which has convergent results for this element number. Also shear stiffnesses in Abaqus  $K_{11}$ ,  $K_{12}$ ,  $K_{22}$  was used in composite section. Values of these stiffnesses are  $A_{44}$ ,  $A_{45}$ ,  $A_{55}$  which were computed with the Matlab code. Also three integration points through the thickness were used as basis.

**Table 5.1** Comparison of Matlab Navier solution and Abaqus fem solution for two layer cross-ply (0/90) square plate under suddenly applied step loading with implicit Newmark method with  $\gamma=0.5$  and  $\beta = 0.25$ , timestep = 1 microsecond

Time (microsecond)	Center Deflection W (cm x 10 <sup>3</sup> )		Central Normal Stress $\sigma_{xx}$ at $z=h/2$ (N/cm <sup>2</sup> )		Shear stress $\sigma_{xz}$ at midside (N/cm <sup>2</sup> )	
	Matlab	Abaqus	Matlab	Abaqus	Matlab	Abaqus
t						
10	0.0077	0.0076	4.036	3.9	0.69	0.67
20	0.0037	0.0367	28.21	27.44	2.26	2.19
40	0.1472	0.1474	113.8	110.2	5.89	5.72
60	0.2922	0.2925	226.9	220.4	12.37	12
80	0.412	0.4119	319.2	309.2	16.34	15.85
100	0.4605	0.4606	357	347	18.94	18.4
120	0.4178	0.4176	323.2	313.2	15.96	16.19
140	0.307	0.306	233.2	225.6	12.58	12.2
160	0.1574	0.1567	119.4	115.7	12.57	12.2
180	0.0417	0.0410	30.6	29.2	6.532	6.32
200	0.0014	0.0014	0.742	0.702	0.56	0.54

As shown in table 5.1 Navier and fem solutions are in agreement each other. Small differences in displacements are due to discretization of spacial coordinates in fem. Also fem is using stresses that is calculated at gauss points then interpolated to nodes.

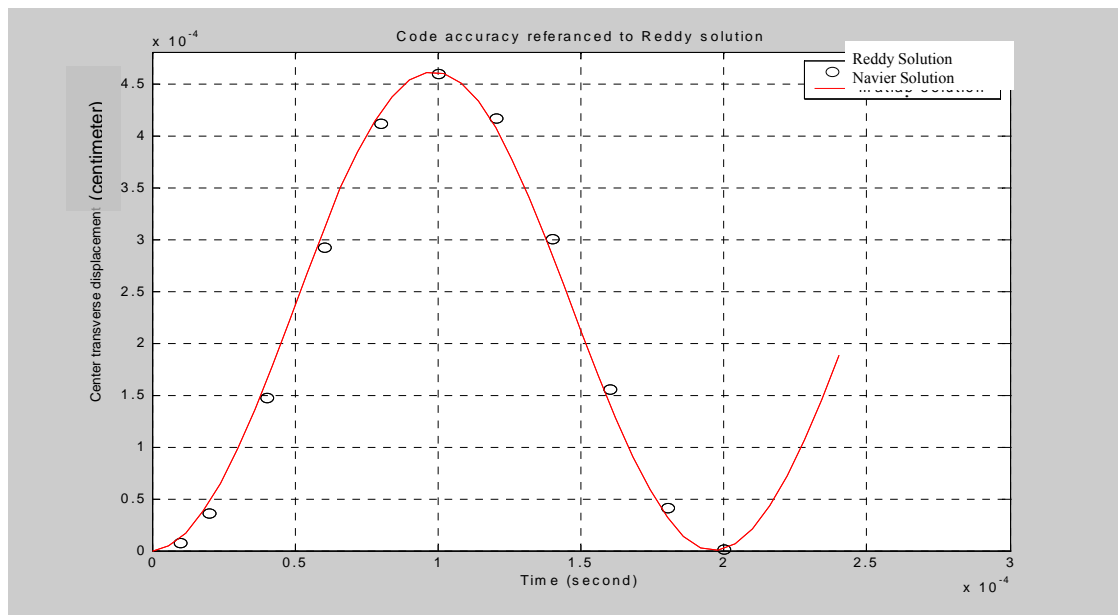


**Figure 5.2** Code accuracy referenced to Reddy's solution [1].

## 5.1 Effect of Time Integration Schemes On Cross Ply Composite Plate

In figure 5.3 and 5.4 central displacement and acceleration behaviour of the plate was shown comparing trapezoidal method and central difference scheme as implicit and explicit solutions. At the time step of 1 microsecond there is good correlation between two solutions.

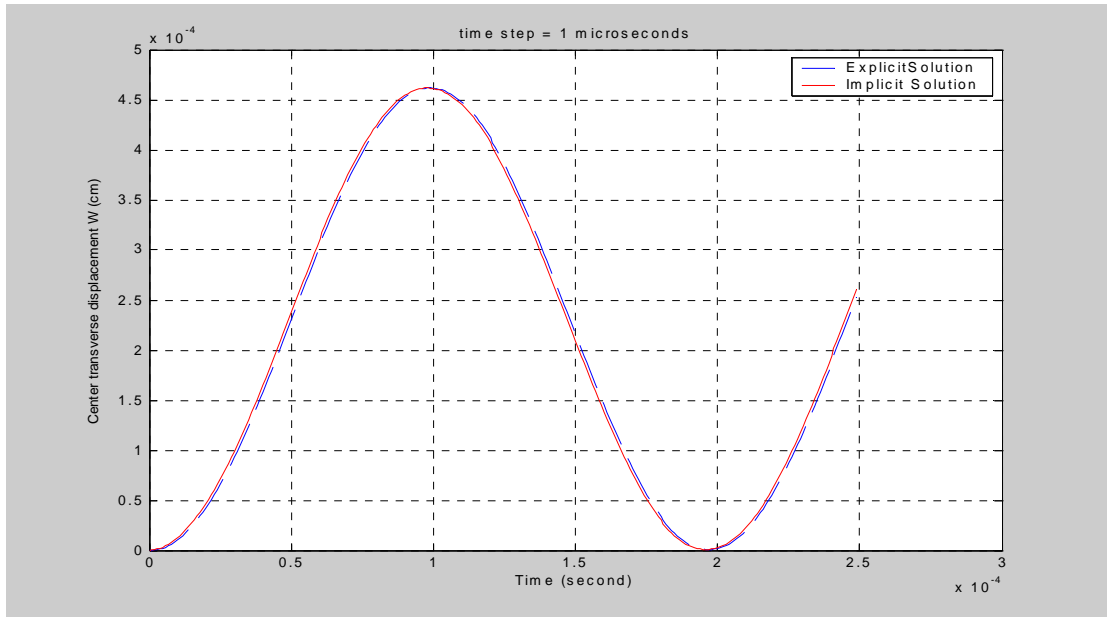


**Figure 5.3** Central Transverse displacement comparison of implicit and explicit schemes with time step 1 microsecond.

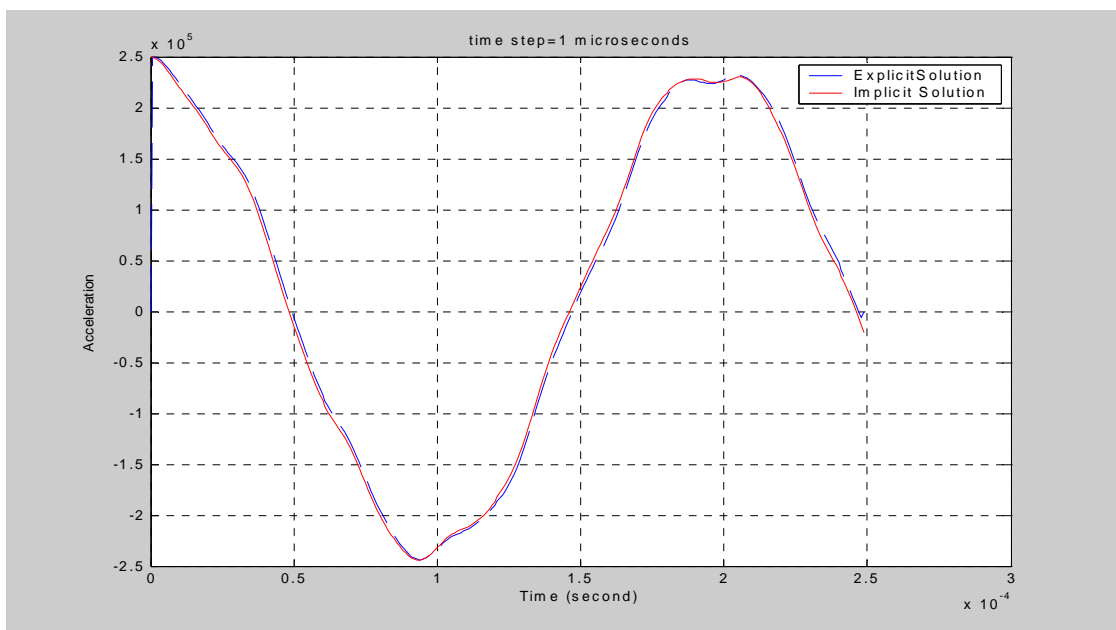


**Figure 5.4** Central transverse acceleration comparison of implicit and explicit schemes with time step 1 microsecond

On the other hand there is considerable deviation in period of the response in explicit central difference scheme with the time step of 5 microsecond as shown in figure 5.5 and 5.6

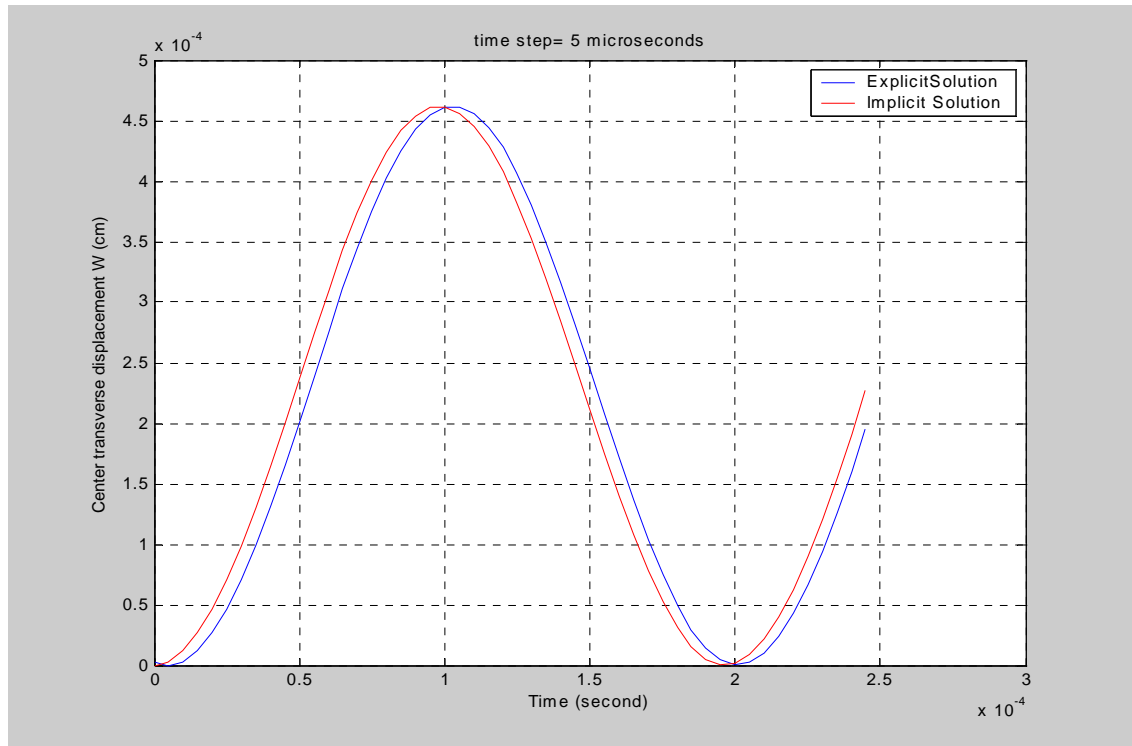


**Figure 5.5** Transverse displacement comparison of implicit and explicit schemes with time step 5 microsecond

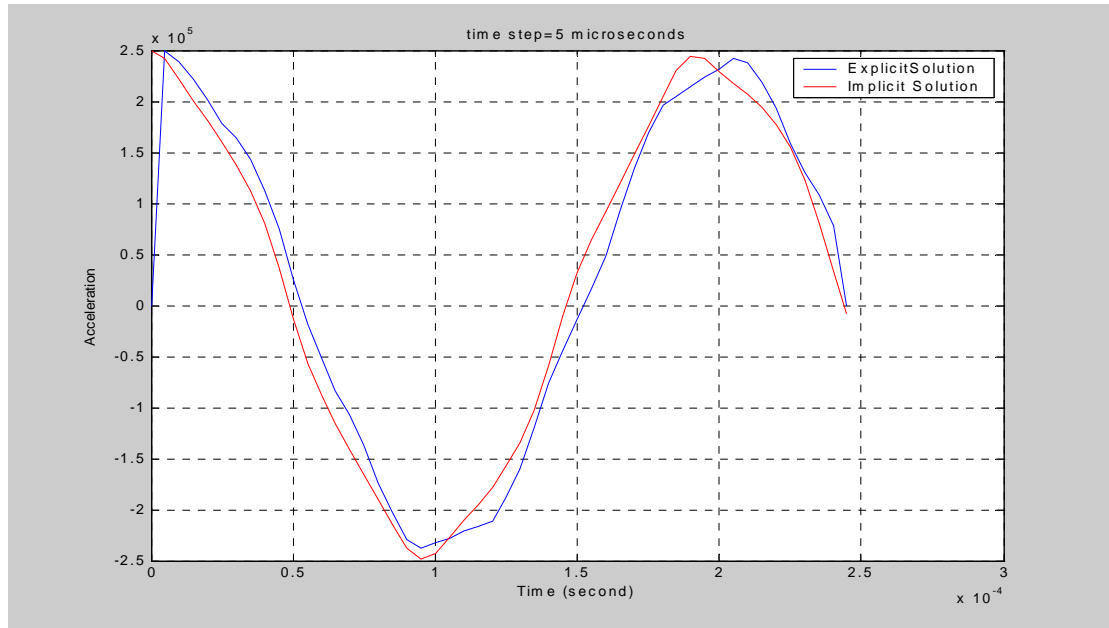


**Figure 5.6** Central transverse acceleration comparison of implicit and explicit schemes with time step 5 microseconds

In trapezoidal scheme solution time step between 1 and 10 microsecond has no appreciable effect on the accuracy of the solution as noted in table 5.2.

**Table 5.2** Effect of Implicit trapezoidal (constant average acceleration) scheme on the transient response of cross ply plate.

time step (microsecond)	0.1	1	5	10	20	25	28	30	50
Max center deflection $w \times 1000$ (cm)	0.46182	0.46183	0.4616	0.4615	0.4613	0.46117	0.455	0.4398	0.4396
Stress $\sigma_{xx}$ (N/cm <sup>2</sup> )	358.2	357.9	351.7	353.8	350	340	112	112	120
period of response(T) (microsecond )	195.4	196	200	200	200	200	224	224	240

Effect of several time steps for the trapezoidal method was shown in figure 5.6 and 5.8. In explicit central difference method, solution instability occurs with the time steps larger than 5 microsecond as shown in figure 5.9. Initiation of instability is at 96 microsecond when time step of 6 microsecond is used. With the increase of time step, initiation of instability shifted to earlier time in transient response as noted in table 5.3.

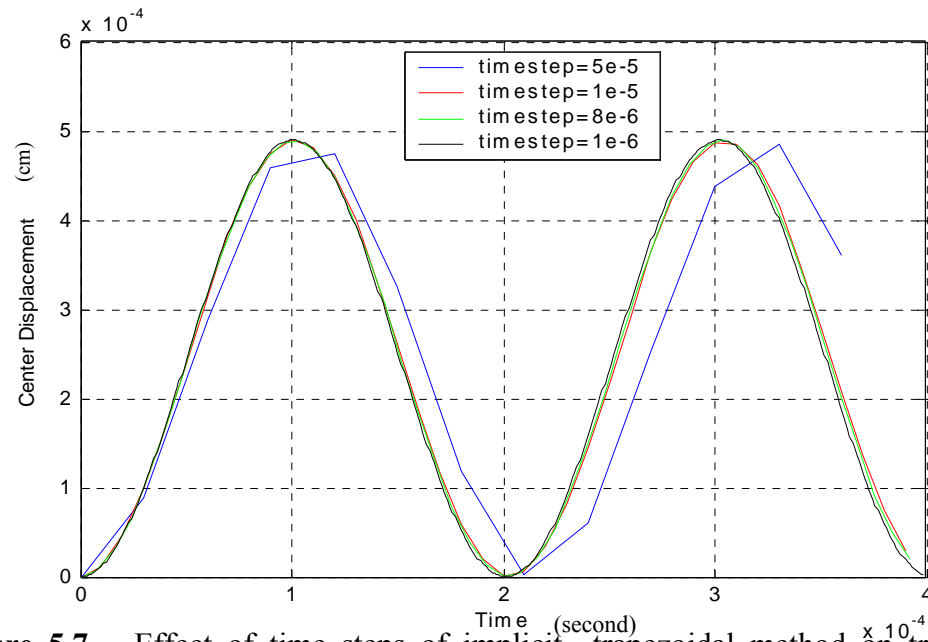


**Figure 5.7** Effect of time steps of implicit trapezoidal method on transverse displacement

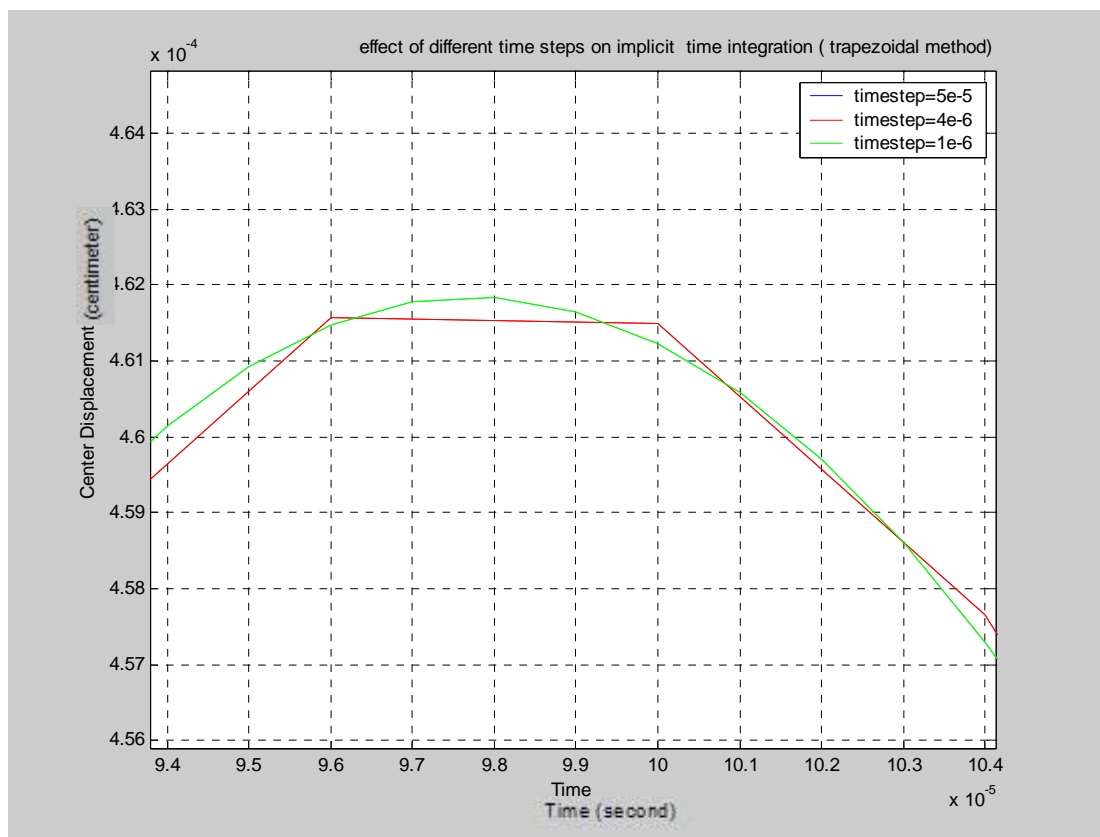


**Figure 5.8** Effect of time steps of implicit trapezoidal method on transverse displacement



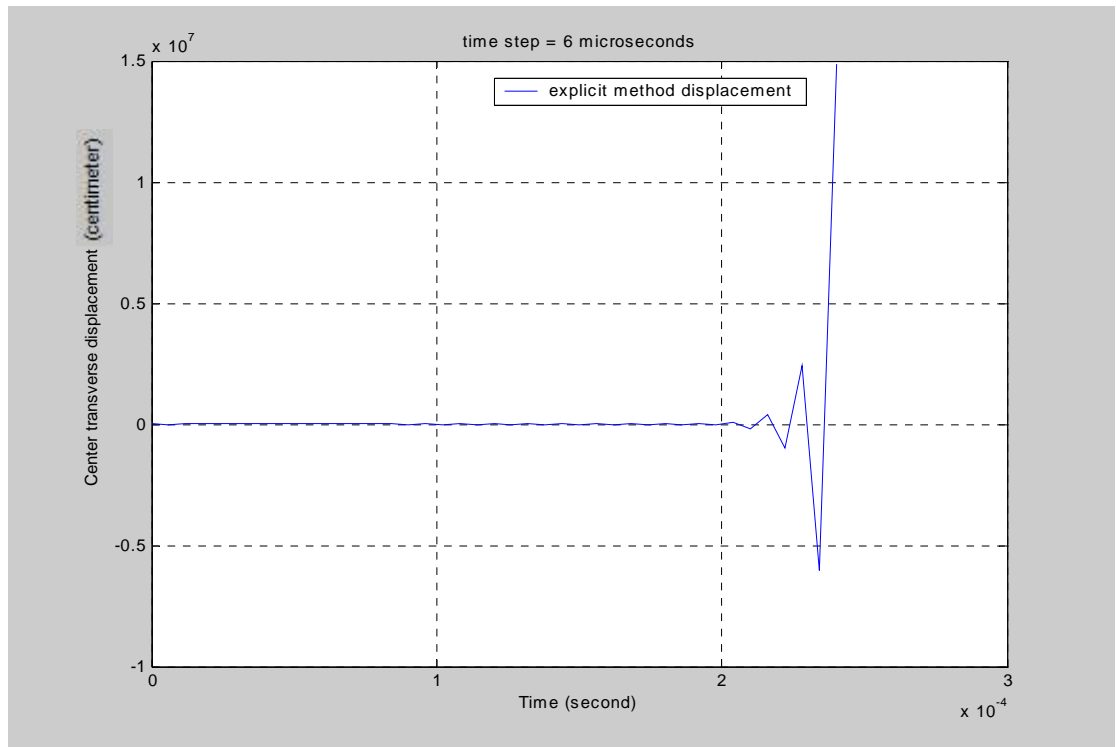


**Figure 5.9** Unstability behaviour of central difference method with time step 6 microseconds

**Table 5.3** Effect of time integration Explicit central difference method with Integration parameters  $\alpha=0.5$   $\beta = 0$  (conditionally stable )

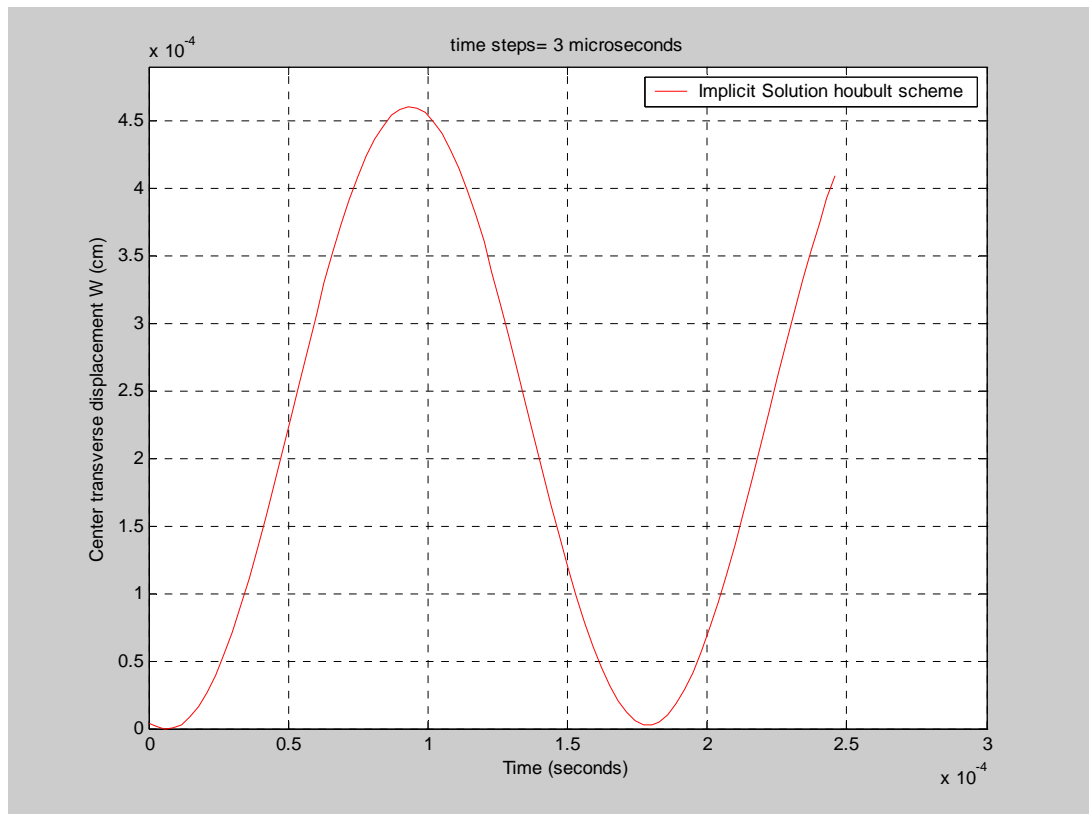
time step (microsecond)	0.1	1	5	6	8	10
Max center deflection $w \cdot 1000$ (cm)	0.46182	0.46180	0.4610	<i>Unstable after</i> 96e-6	<i>Unstable after</i> 56e-6	<i>Unstable after</i> 40e-6
Normal Stress $\sigma_{xx}$ (N/cm <sup>2</sup> )	358.2	357.3	355			
period of response(T) (microsecond)	195.6	198	210			

Houbolt scheme is addressed the amplitude of the response accurately with the time step 0.1 microsecond and 1 microsecond however there is considerable differences in the period of response with in these time steps as noted in table 5.4 . Also the effect of time step on the accuracy of the displacement and stress solutions after 3 microseconds is appreciable in this method.

**Table 5. 4** Effect of time integration with houbolt implicit scheme

time step (microsecond)	0.1	1	3	6	20
Maxcenter deflection $w*1000$ ( cm)	0.46182	0.4617	0.4602	0.4559	0.4154
Normal Stress $\sigma_{xx}$ (N/cm <sup>2</sup> )	361	360	128	123	110
period of response(T) (microsecond )	170	174	216	228	320

Another issue observed in Houbolt method is the amplitude decay as shown in figure 5.10 and 5.11. This amplitude decay is increasing with the larger time steps. At 10 microseconds it is about the 4 percent of the first peak a shown in fig 5.12.

**Figure 5.10** Effect of Houbolt time integration on transient response

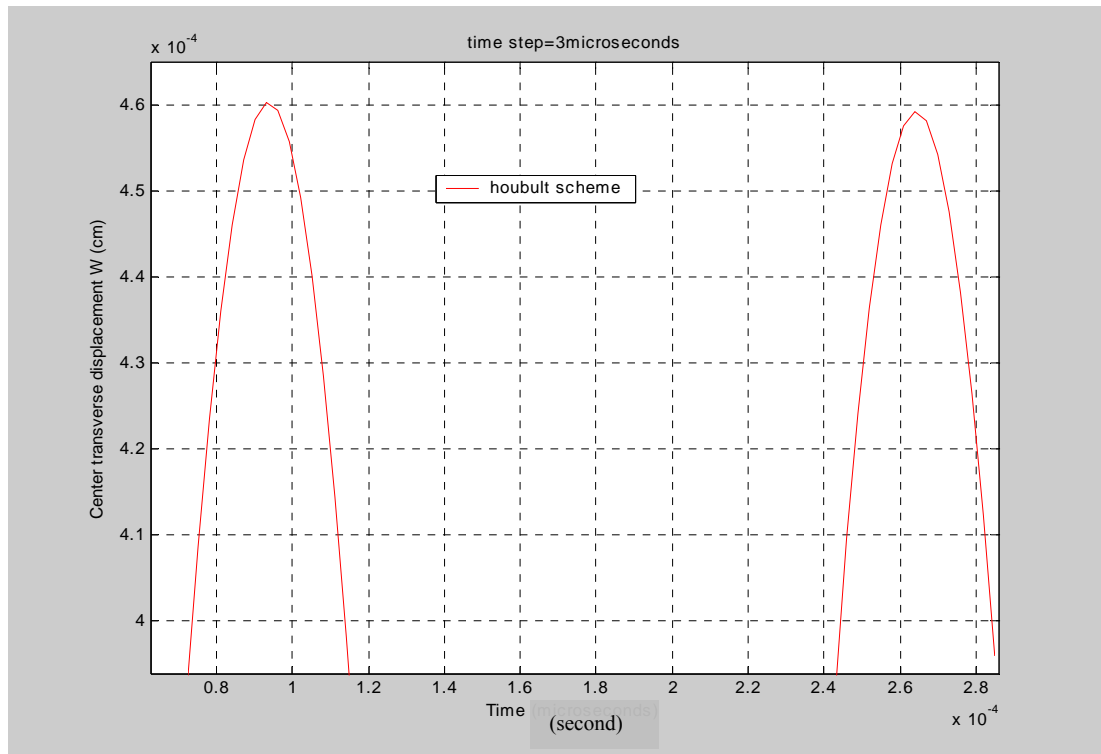


**Figure 5.11** Effect of numerical damping of Houbolt time integration scheme

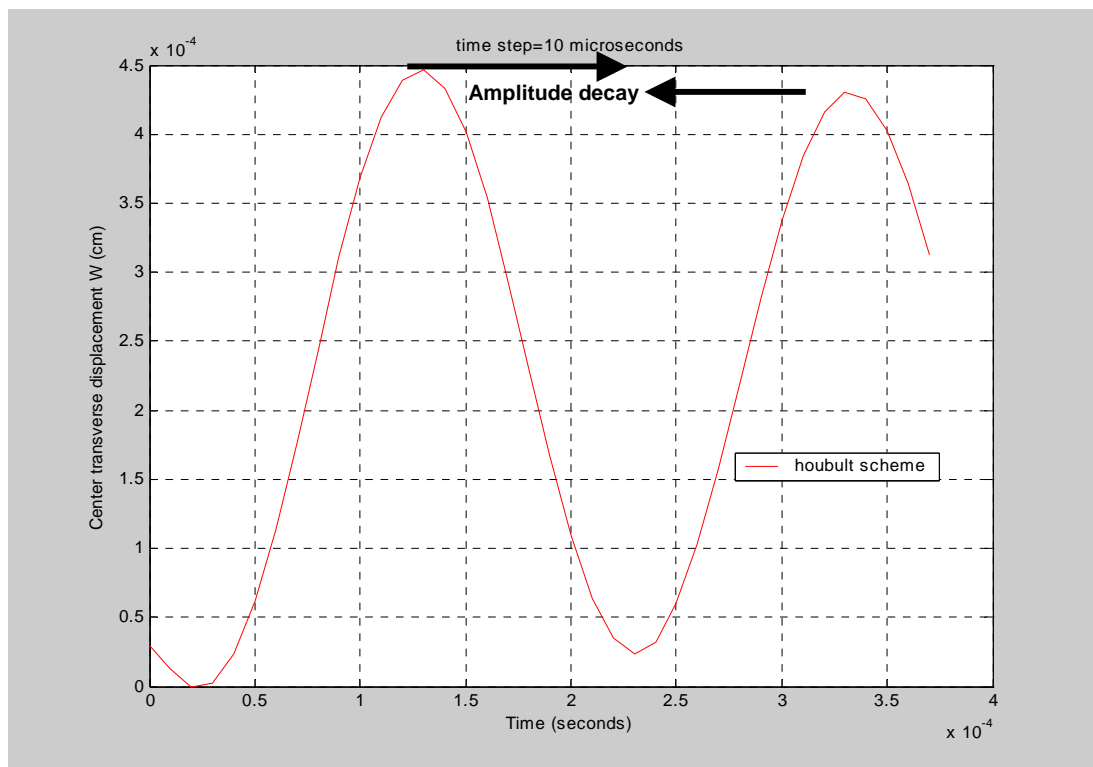


**Figure 5.12** Effect of numerical damping of Houbolt time integration scheme at time step 10 microseconds.

## 5.2 Effect of Plate Theories On The Transient Response

Investigation of the effect of plate theories clearly show that classical theory underpredict the maximum displacement and stress as shown in figure 5.12 and 5.13

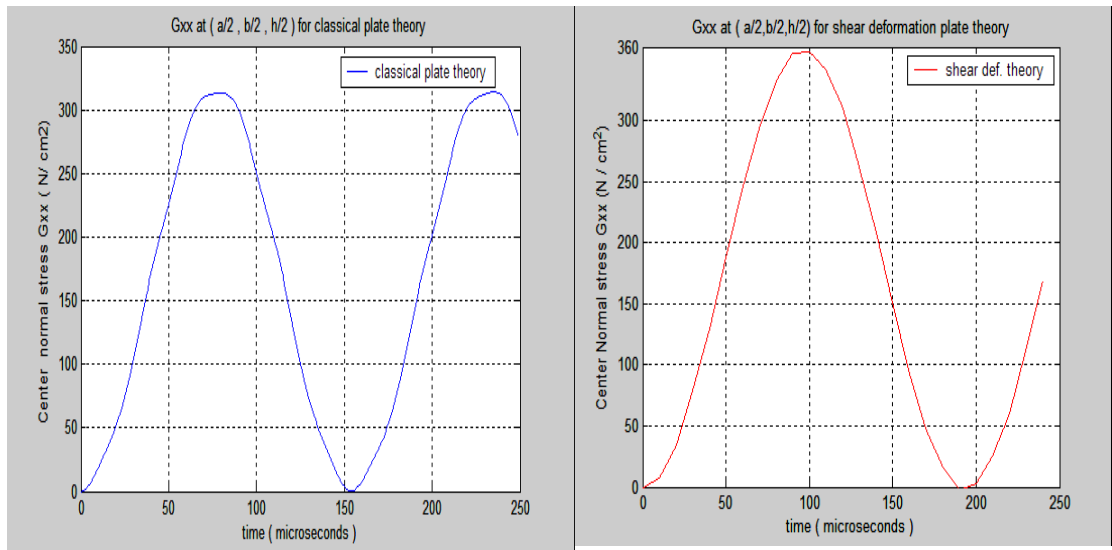


**Figure 5.13** Center normal stress for classical and shear deformation theory

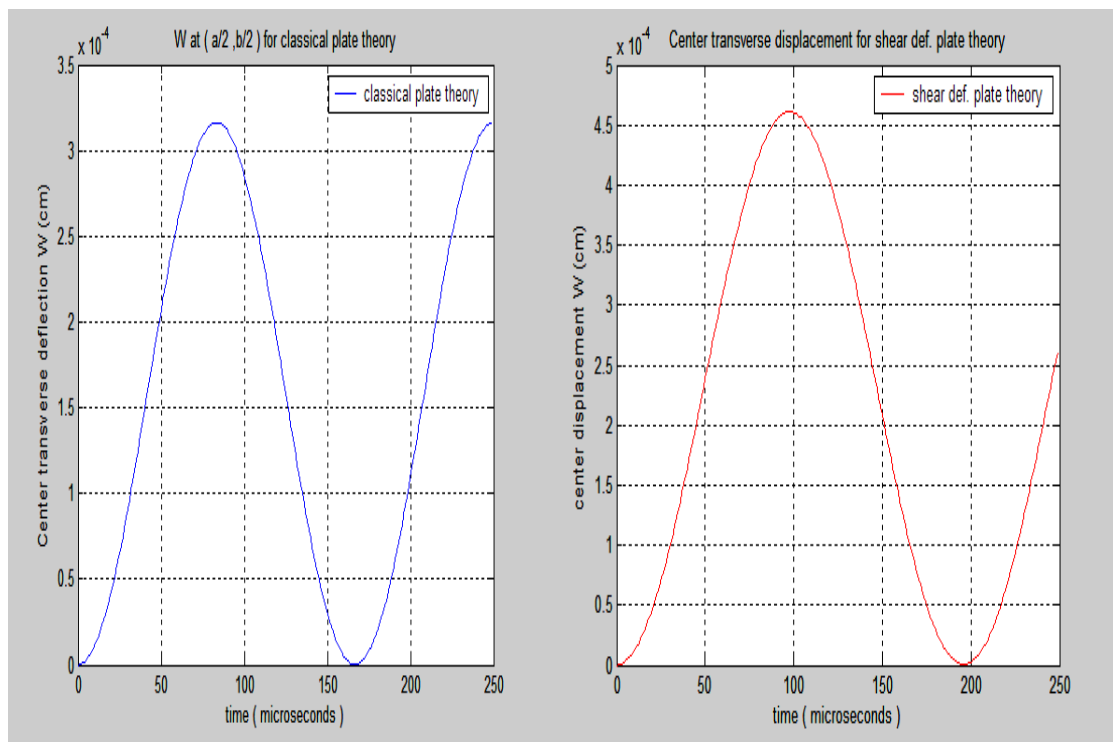


**Figure 5.14** Center transverse displacement for classical and shear deformation theory

Also classical theory overpredicted frequency of the response when length thickness ratio ( $a/h$ ) is 5 as noted in table 5.5 and 5.6.

**Table 5.5** Effect of classical plate theory on the response of two layer cross ply plate

time step (microsecond)	0.1	1	5	10	25
Max center deflection $w*1000$ (cm)	0.3162	0.3162	0.3160	0.3140	0.3051
In plane stress $\sigma_{xx}$ (N/cm <sup>2</sup> ) at $z=-h/2$	-0.8725	-0.8716	-0.8711	-0.8704	-0.8356
period of response(T) (microsecond)	166	166	170	160	200

**Table 5.6** Effect of shear theory on the response of two layer cross ply plate.

time step (microsecond)	0.1	1	5	10	25
Maxcenter deflection $w*1000$ (cm)	0.4618	0.4618	0.4616	0.4615	0.46117
In plane stress $\sigma_{xx}$ (N/cm <sup>2</sup> ) $z=-h/2$	-0.8909	-0.89	-0.8858	-0.8849	-0.8831
period of response (microsecond)	195.4	196	200	200	200

It is also observed that shear deformation theory is less sensitive to time step compared with the classical plate theory in this range. Considering the effect of number of layers on transient response of the composite plate, considerable large deflection was observed in two layer cross ply composite plate configurations compared to single and multiple configurations as shown in table 5.7. Also ten to twenty percent smaller frequency was addressed in two layer configuration compared to other configurations.

**Table 5.7** Effect of layers and shear deformation on the center transverse deflection and period of simply supported cross ply(0/90/.....) composite square plates for a/h=5.

LaminationScheme (0/90/...)	1	2	3	Layers 4	5	6	7	8	
Classical plate theory	0.128	0.3153	0.128	0.1493	0.128	0.1336	0.128	0.1325	deflection*10 <sup>3</sup> (cm)
	110	170	110	120	110	110	110	110	period(microsecond)
Shear deformation plate theory	0.3556	0.4605	0.3378	0.295	0.292	0.281	0.283	0.276	deflection*10 <sup>3</sup> (cm)
	180	200	170	160	160	160	160	140	period(microsecond)

### 5.3 Verification of Transient Matlab Code with Sample Literature Problems and Evaluation on The Geometric Nonlinearity Effect in Plates.

For the verification of the Navier solution based linear transient Matlab code, two problems from the article of the J.Chen [20] were solved with the code. Also geometric nonlinearity effect was issued.

First thin isotropic plate was considered with a side length a=b= 508 mm and thickness of 3.4 mm. Material properties used in the analysis,

E= 206840 MPa, density =7900kg/m<sup>3</sup> , poison ratio =0.3.

The plate is subject to the blast loading which has uniform intensity over the whole plate at any instant of time, but this intensity varies with time as shown in figure 5.15.

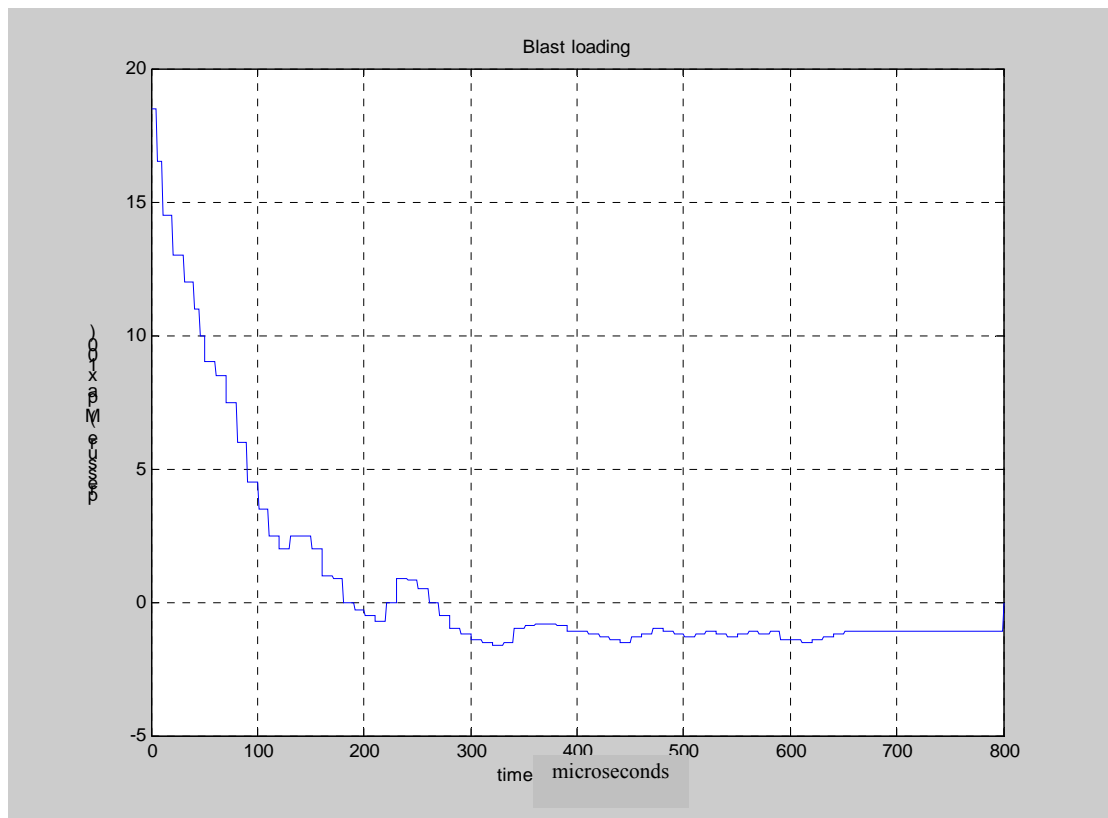


**Figure 5.15** Uniformly distributed blast pressure - time history for isotropic plate

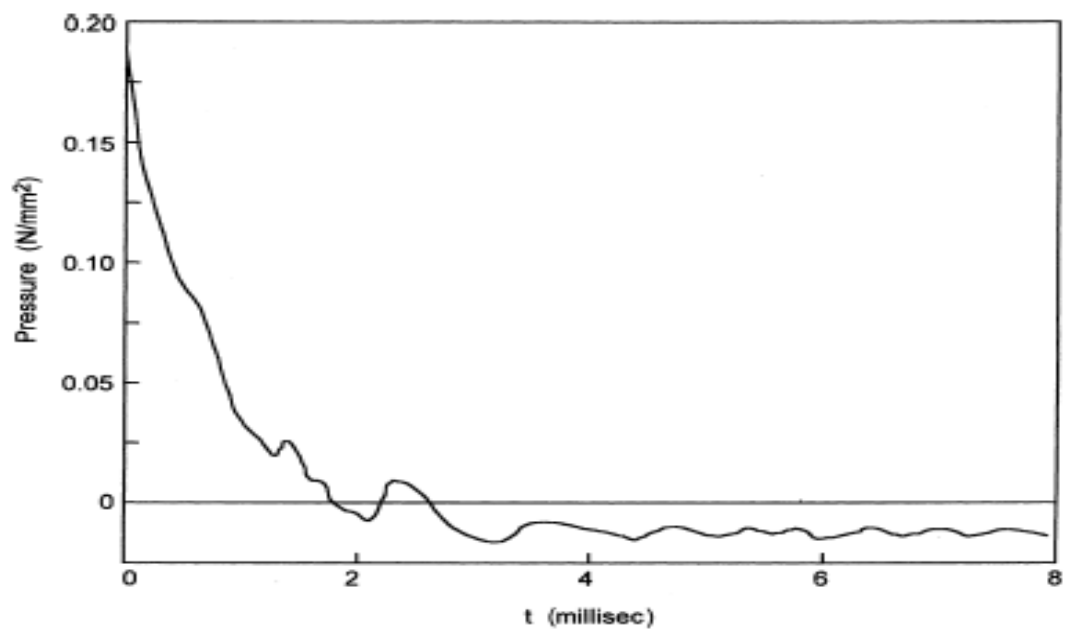


**Figure 5.16** Blast Pressure versus time for sample problem of Chen [20].

Time dependency of loading used by Chen is shown in figure 5.16. In Matlab this uniform loading is applied as step loading within the interval of 10 microseconds. This is the only difference regarding the original loading of Chen.

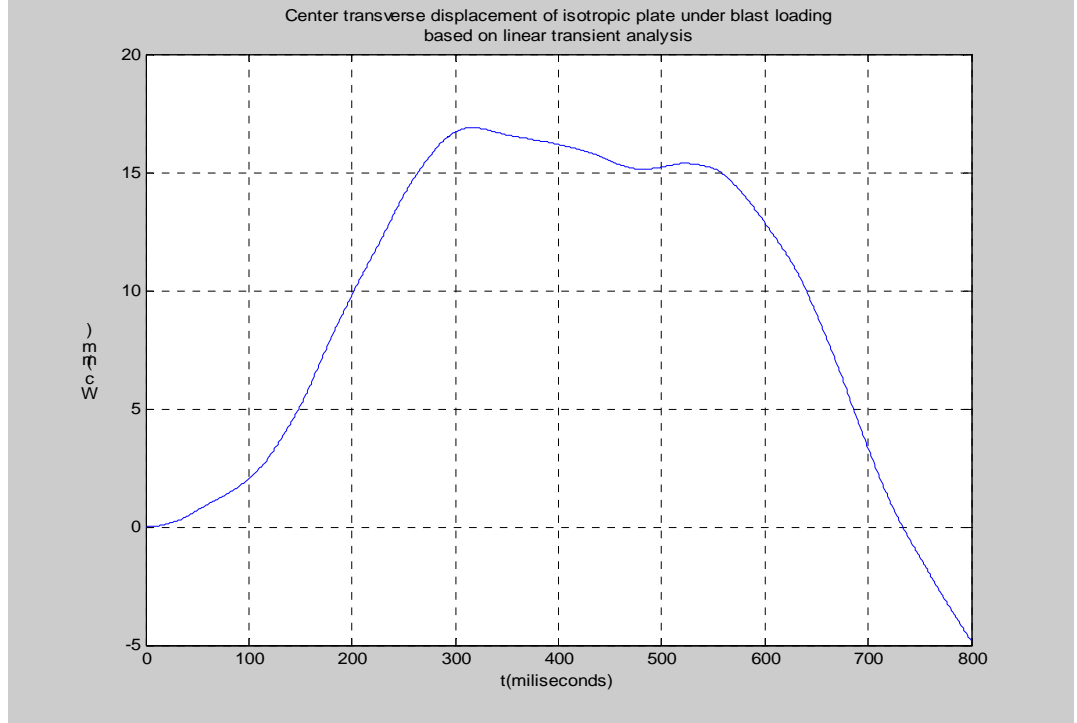


**Figure 5.17** Response of isotropic plate to blast pressure central deflection

Good correlation was observed for linear transverse displacement ( figure 5.17 ) compared with the linear finite strip solution of the Chen ( figure 5.18 ).

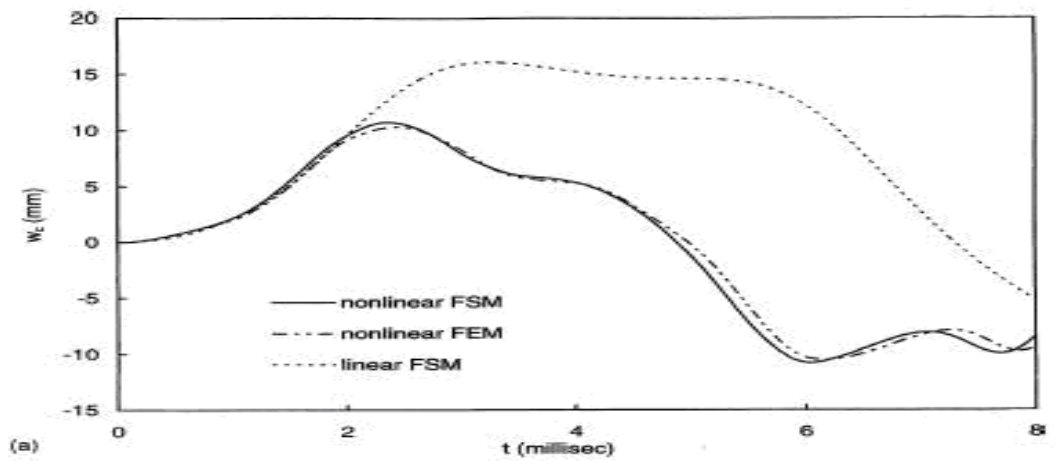


**Figure 5.18** Chen's [20] linear and nonlinear results with finite element and finite strip method for the response of isotropic plate to uniform blast pressure central displacement



Also good correlation was obtained in central normal stress at upper side of the plate as shown in figure 5.19 and 5.20.

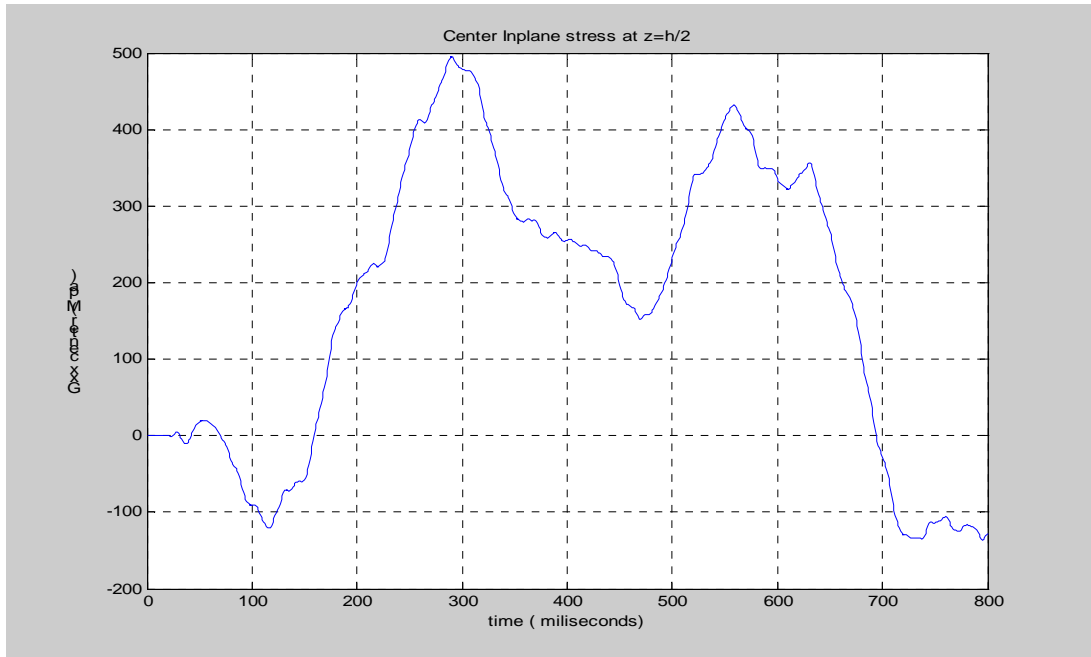


**Figure 5.19** Response of isotropic plate to blast pressure central in plane stress

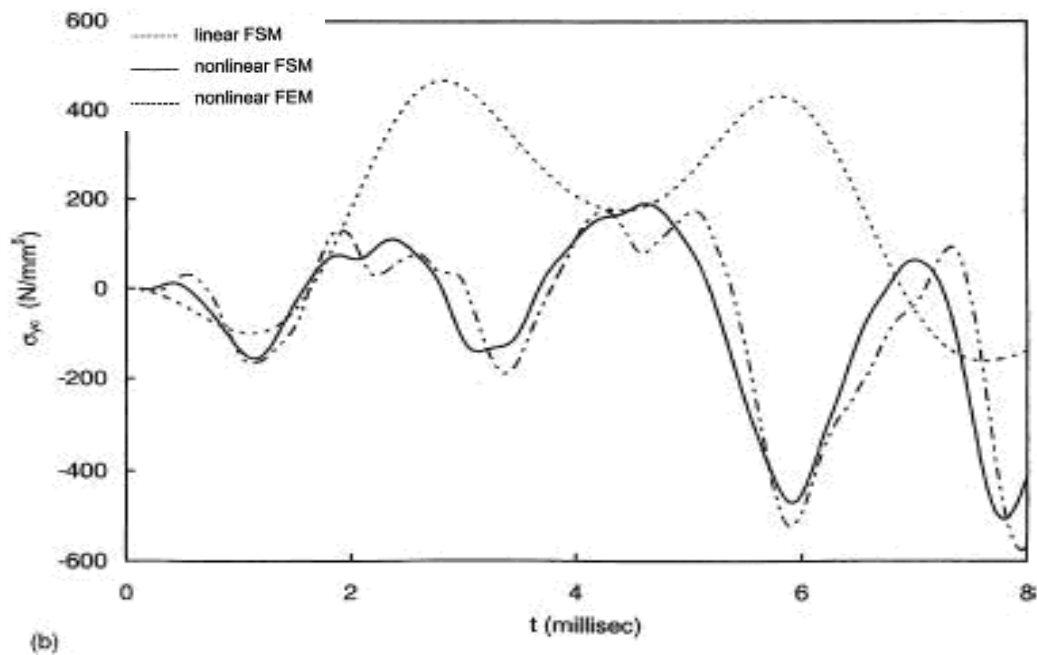


**Figure 5.20** Chen's [20] linear and nonlinear results with FEM and FSM

It is also addressed due to large geometric transverse displacement about the 3th times thickness, geometric nonlinearity should be included for the first case

In the second case, one layer orthotropic plate with uniform step loading was considered. Geometric dimensions for side lengths are 250 mm, thickness is 5mm and intensity of the load is 0.1 MPa. Orthotropic material properties are as follows

$$E_1 = 525\,000 \text{ MPa}, E_2 = 21\,000 \text{ MPa}$$

$$G_{12}=G_{13} = G_{23} = 10500 \text{ MPa}$$

$$\nu_{12}=0.25, \rho=800 \text{ kg/m}^3.$$

For uniform loading coefficients in the double trigonometric series expansion of loads in the navier method,

$$Q_{mn} = -16 q_0 / \pi^2 m n \quad (m, n = 1, 3, 5, \dots) \quad , \quad q_0 : \text{load intensity} \quad (4.14)$$

In this study upper limit of m and n are 20. So computations are including two hundred terms for accuracy consideration.

As shown in figure 5.21 and 5.23, dimensionless displacement and stress response of plate is in agreement with solution of Chen's [20] in figures 5.12 and 5.24. In this load intensity it is also observed that there is no considerable change in linear and nonlinear geometric approaches. This result could be predicted from the maximum dimensionless displacement value which is  $w/h = 0.43$ . So when displacement is 0.43 times the thickness, it could be accepted as in the linear range so small rotations assumptions in bending still works and gives close results to the geometric nonlinear approach.

For small deflections ( $w \leq 0.2 h$ ) linear plate theory gives sufficiently accurate results. By increasing the magnitude of the deflections beyond the certain level ( $w \geq 0.3 h$ ) however the lateral deflections are accompanied by stretching the middle surface. The membrane forces produced by such stretching can help appreciably in carrying the lateral loads. If the plate, for instance, is permitted to deform beyond half its thickness, its load-carrying capacity is already significantly increased. When the magnitude of the maximum deflection reaches the order of the plate thickness ( $w \approx h$ ), membrane action predominates. Consequently, for such problems, the use of an extended plate theory which accounts for the effects created by large deflections is mandatory [24].

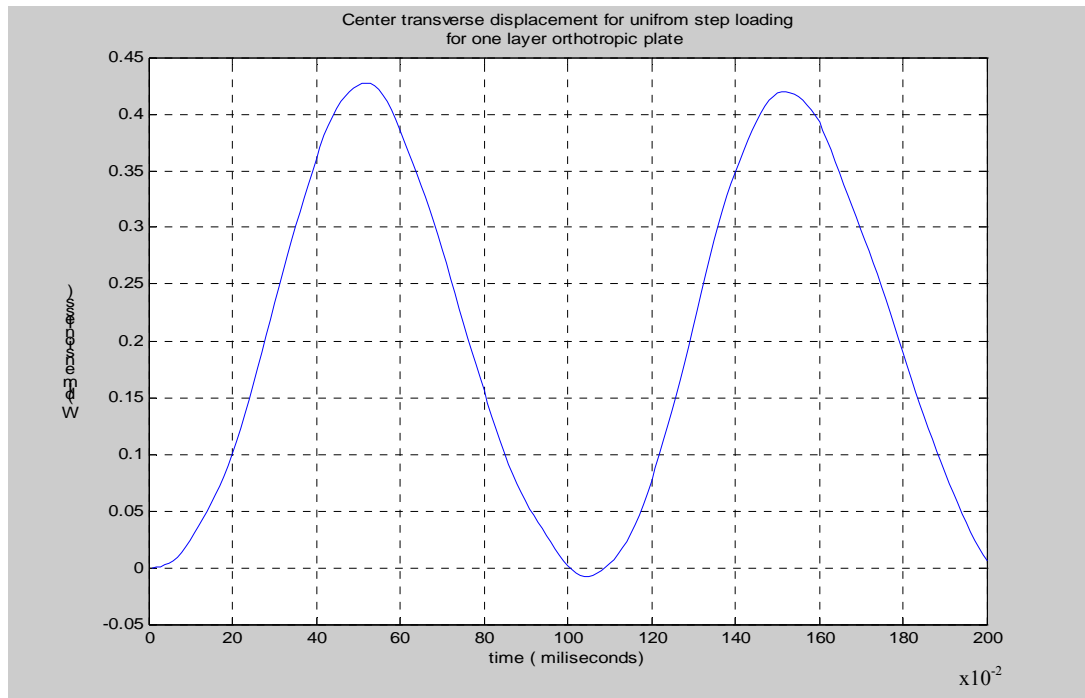


**Figure 5.21** Central transverse displacement response of one layer orthotropic plate subject to uniform step loading

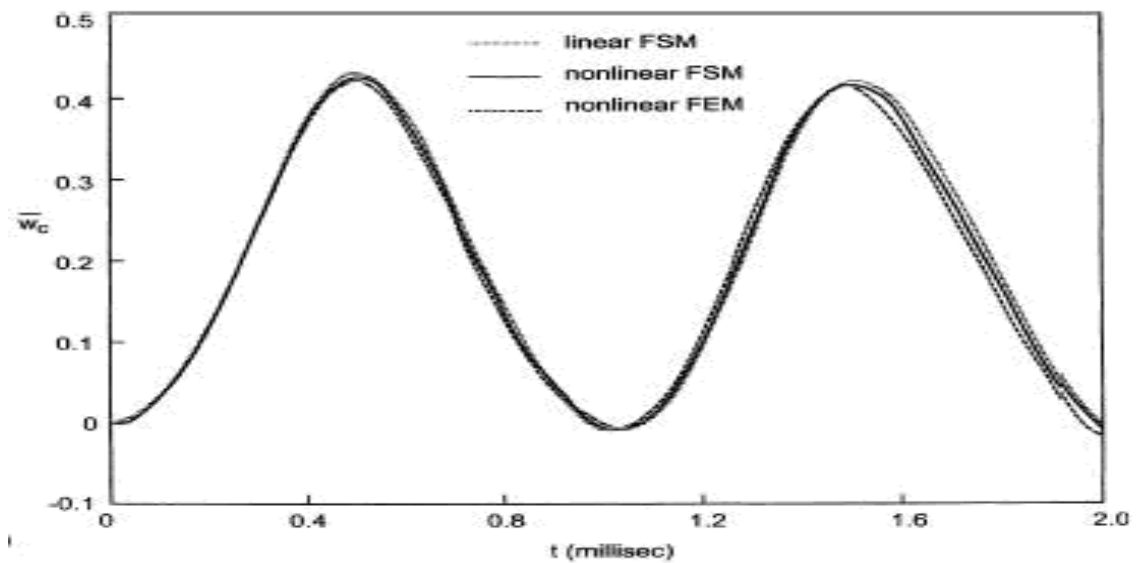


**Figure 5.22** Chen's [20] linear and nonlinear results with finite element and finite strip method for the response of one layer orthotropic plate to uniform step loading with central displacement – time response.

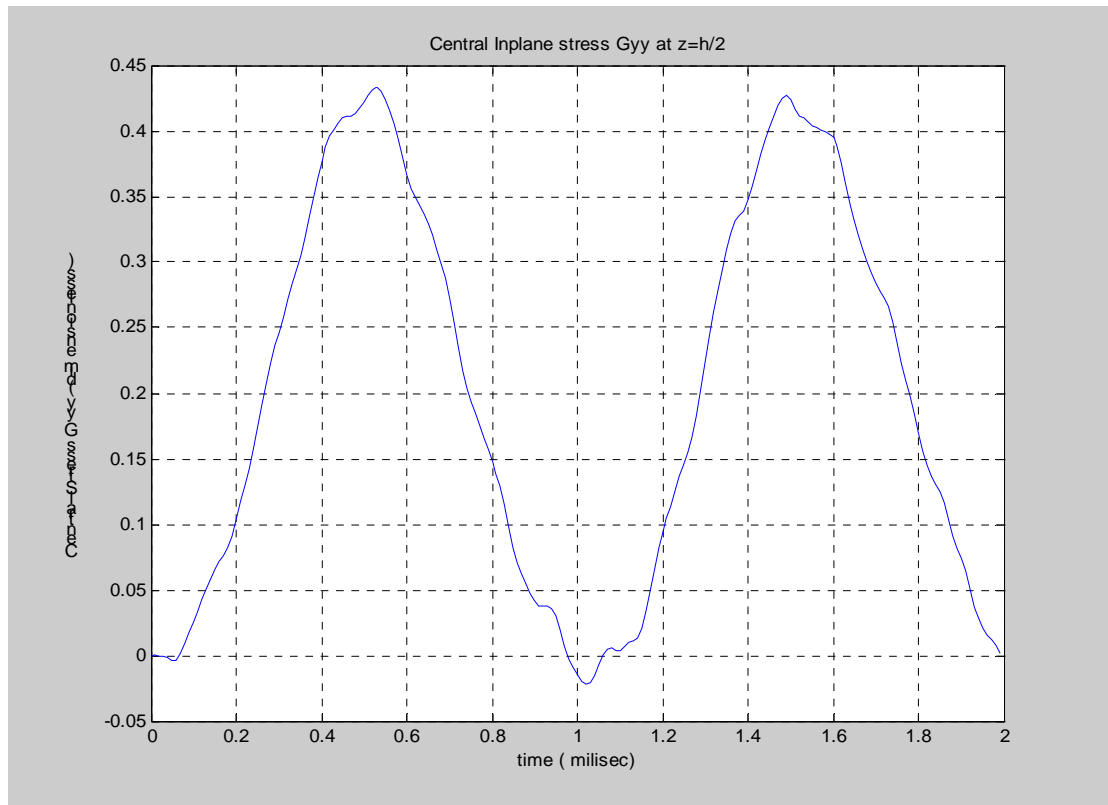


**Figure 5.23** Central in plane stress of one layer orthotropic plate subject to uniform step loading

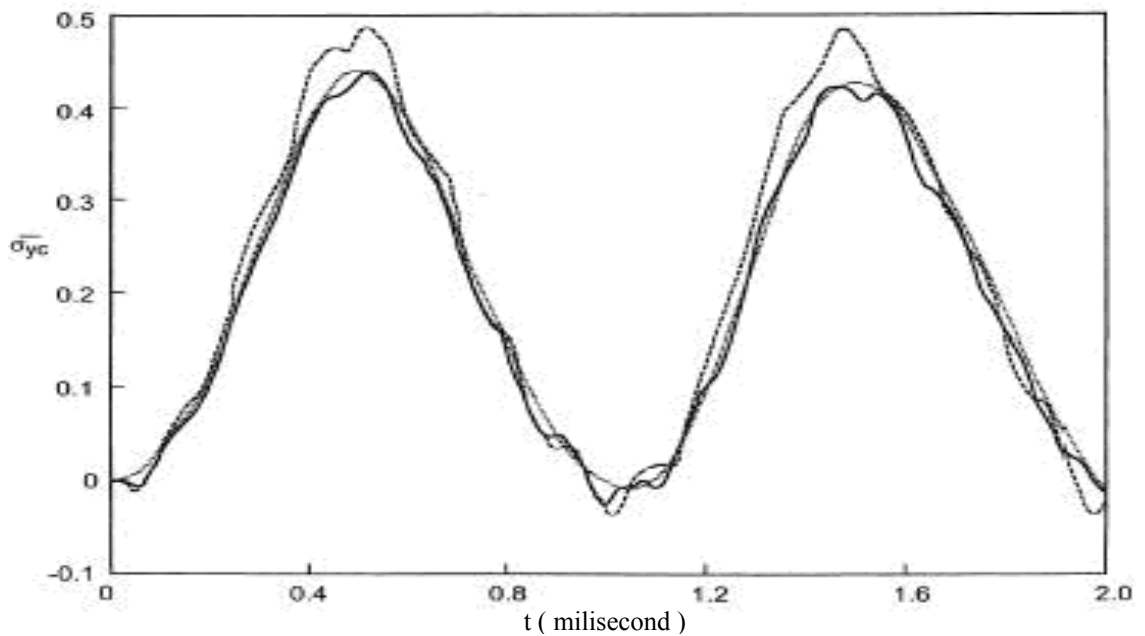


**Figure 5.24** Chen's [20] linear and nonlinear results with finite element and finite strip method for the response of one layer orthotropic plate to uniform step loading with central stress –time at upper side of the plate.

## 7. CONCLUSIONS AND RECOMMENDATIONS

Transient analysis of composite plates has an important area of application in aerospace and ballistic industry. Response of composite plates to drop, impact and blast type of loadings is influential factor in design consideration. Thus in last years several numerical solution techniques are developed and investigated to address this type of response. Especially many finite element code exist in the commercial market with implicit and explicit dynamic solvers. In this thesis, the Navier solution technique was programmed with Matlab code to investigate the linear transient response of cross ply composite plates. Effects of implicit and explicit time integrations techniques were addressed. Also accuracy, stability and time step sensitivity of these methods were outlined considering period elongation and amplitude decay in displacement and in plane stress response. Effect of shear deformation plate theory and number of layers on transient response of cross ply composite plate is presented.

The results clearly show that trapezoidal implicit method ( Newmark method with  $\gamma=0.5$  and  $\beta = 0.25$  ) has better approximation in time space in terms of accuracy and stability. It has no amplitude decay in response. Also this method gives advantage of using larger time steps without sacrifice on the accuracy of the solutions. In Houbolt scheme and explicit central difference scheme deviation from the accuracy of the solutions were observed at larger time steps compared with trapezoidal method. Although explicit scheme has good correlation at smaller time steps, it suffers instability with time steps larger than 5 microseconds. So conditional stability of this method is important problem at these time steps. This may result in storage problems during the solution. Houbolt method is the most sensitive method to time steps considered. It has shown serious inaccuracy in the considered time step range compared with trapezoidal and central difference schemes. Also considerable period elongation and numerical damping was observed in the transient response for low mode of response. So Houbolt is inappropriate time integration technique for short duration dynamic problems.

In the considered  $a/h$  ( $a/h=5$ ) ratio, thirty percentage of difference was observed in displacement response when shear deformation theory is used in plate behaviour. Although this ratio is so severe classical plate theory under predict the displacement and stress response while over predict the frequency of the response. Difference in results between two theory is lessening with the increase of  $a/h$  ratio. It is also addressed that shear deformation theory is less sensitive time step in transient dynamic problems compared with classical theory. As a result of the investigation on the effect of number of layers, considerable large deflection was observed in two layer cross ply composite plate configurations compared to single and multiple configurations. Also ten to twenty percent increase in frequency was addressed in two layer configuration compared to other configurations.

## REFERENCES

- [1] **Reddy J.N., 1982**, On the solutions to forced motions of rectangular Composite plates, Journal of Applied Mechanics, **49**, 403-407.
- [2] **Reddy J.N., 1986**, Mechanics of composite plates & Theory and Analysis , Department of Mechanical Engineering Texas A&M Univeristy , Texas.
- [3] **Reisman.H., 1968**, Forced motions of elastic plates , Journal of Applied Mechanics, **35**, 510-568.
- [4] **Rock,T., and Hinton E., 1974**, Free vibration and transient response of thck and thin plates using the fem, Earthquake Engineering and Structural Dynamics,**3**, 51-63.
- [5] **Bathe K.J., Wilson E.L, 1973**, Stability and accuracy analysis of direct integration methods, Earthquake Engineering and Structural Dynamics , **1** , 283-291.
- [6] **Belytschko T., Hughes T., 1983**, Computational methods for transient analysis, First series of computational mechanics , North – Holland.
- [7] **Anderson T., Madenci E., 1997**, Analytical Solution of finite geometry composite panels under transient surface loading , International Journal of Solid and Structures , **35**, 1219-1239.
- [8] **Y.Li , Ramesh K.T., Chin E.S., 2001**, Dynamic caharacterization of layered and graded structures under impulsive loading, International Journal of Solid and Structures, **38**, 6045-6061.
- [9] **Dobyns A.L, 1980**, Analysis of simply supported orthotropic plates subject to static and dynamic loads , AIAA,19, No.5.
- [10] **Sun C.T., Chattopadhyay, 1975**, Dynamic response of Anisotropic Laminated plates under Initial Stress to impact of a Mass , Journal of Applied Mechanics, **5**, 693-698.
- [11] **Whitney J.M, Pagano N.J, 1970**, Shear deformation in the heterogeneous anisotropic plates, Journal of Applied Mechanics, **128**, 1031-1036.
- [12] **Srivinas S., Rao A.K., 1970**, Bending ,vibration and buckling of simply supported thick orthotropic rectangular plates and laminates, International Journal of Solid and Structures **6**, 1463-1481.

- [13] **Moon, F.C., 1973**, One dimensional transient waves in anisotropic plates. Journal of Applied Mechanics, **40**, 485-490.
- [14] **Whitney J.M., 1987**, Structural analysis of laminated anisotropic plates, Air Force Material Laboratories Patterson Air Base , Dayton , Ohio.
- [15] **Subbaraj K., Dokainish M.A., 1998**, A Survey Of Direct time Integration methods in computational structural dynamics – I . Explicit methods, Computers and Structures ,**32**, 1387-1401.
- [16] **Subbaraj K., Dokainish M.A., 1998**, A Survey Of Direct time Integration methods in computational structural dynamics – II . Implicit methods , Computers and Structures ,**32**, 1371-1386.
- [17] **Chow T.S, 1971**, On the propagation of flexural waves in an orthotropic laminated plate, Journal of compoiste materials , **5**, 306-319.
- [18] **Sun C.T, 1973**, Propagation of shock waves in anisotropic composite plates Journal of composite materials,**7**, 366-382.
- [19] **Mal.A.K., Lih.S., 1992**, Elastodynamic response of a unidirectional compoiste laminate to concentrated surface loads. Journal of Applied Mechanics,**59**,878-892.
- [20] **Chen J., Dawe D.J., 2000**, Nonlinear transient analysis of the rectangular composite plates .Journal of Composite Materials ,**49**,129-139.
- [21] **Argyrs .J., 1991**, Dynamics of Structures,Texts on computational mechanics volume 5, North-Holland(1991).
- [22] **T. Belytschko, W. K. Liu, and B. Moran**, Nonlinear Finite Elements for Continua and Structures, Wiley (2000).
- [23] **Kanchi .M.B**, Matrix Method of Structural Analysis, Wiley(1983).
- [24] **Rudolph Szilard**, Theory and Analysis of Plates, Prentice Hall (1974).



## **BIBLIOGRAPHY**

Kıvanç Şengöz was born in Nazilli at 1978. He enrolled Aeronautical and Aerospace Department at Istanbul Technical University in 1997. He was graduated in 2001. He led his professional career at FIGES A.Ş three years as a senior finite element analyst. His master education at Solid Mechanics Program of the Mechanical Engineering Department in ITU is going on.